

Simultaneously determine elastic impedance and shape by a Newton-type iterative method

Yao Sun*, Pan Wang

sunyao10@mails.jlu.edu.cn

College of Science, Civil Aviation University of China, Tianjin, China

Abstract. This paper focuses on the inverse elastic impedance and the geometry problem by a Cauchy data pair on the access part of the boundary in a two-dimensional case. Through the decomposition of the displacement, the problem is transform the solution of into a coupled boundary value problem that involves two scalar Helmholtz equations. Firstly, a uniqueness result is given, and a non-iterative algorithm is proposed to solve the data completion problem using a Cauchy data pair on a known part of the solution domain's boundary. Next, we introduce a Newton-type iterative method for reconstructing the boundary and the impedance function using the completion data on the unknown boundary, which is governed by a specific type of boundary conditions. Finally, we provide several examples to demonstrate the effectiveness and accuracy of the proposed method.

Key words: Inverse elastic impedance, Elastic wave, Collocation method.

1 Introduction

The study of elastic waves has become an important research area in mathematical physics. This type of problem is widely used in nondestructive testing, medical imaging, and seismic exploration [3, 4, 10, 11]. A typical inverse problem involves determining the boundary shape of an elastic obstacle from the Cauchy data on the accessible part boundary. In practical applications such as physics and engineering, due to multiple factors including measurement technology limitations, it is not possible to obtain complete information about the surface of obstacles. Therefore, it is necessary to consider supplementing the information about the non-accessible part boundary. In the case of electrostatics, the model yields an inverse boundary value problem related to the Laplace equation. In the case of elastic obstacles, an inverse boundary value problem arises in relation to the Navier equation. Literature references can be consulted for both cases [1, 14, 22, 31].

Various methods have been investigated in recent years to solve the inverse elastic obstacle problem. For instance, Louër [28, 29] derives the domain derivatives of elastic scattering, which can be employed to reconstruct unknown elastic

obstacles through the design of gradient descent methods. Additionally, Alves and Kress [2] examine a linear sampling method, which is based on far-field operator decomposition, for inverse elastic scattering problem. Factorization method has been extensively researched by Hu et al. in [18, 19]. The inverse elastic impedance problem, as discussed in [26, 38], has found widespread application in seismology, oilfield exploration, and other related fields. There are some other research papers for the inverse elastic problem, such as [15, 27] and etc.

In this paper, we aim to demonstrate a Newton-type iterative method for reconstructing the elastic impedance function and the shape of the elastic body based on the integral equations. Additionally, we propose a regularization method to remove the noise. When solving the inverse problem, it can be decomposed into two problems. The first is a severely ill-posed linear problem, while the second is a slightly ill-posed nonlinear problem. This decomposition approach has been utilized in some inverse problems [7, 24], offering numerous advantages. One notable advantage is that the forward problem does not need to be solved at each iteration, resulting in a significant reduction in computational cost. Furthermore, the Fréchet derivative of the boundary integral operator is represented as an integral operator. This technique can be found in [9, 12, 17, 25] and the literature cited therein.

The paper is organized as follows. In Section 2, we introduce the inverse impedance problem and the inverse shape problem. In Section 3, some theoretical results including a unique result are given by introducing the Helmholtz decomposition of the displacement. Then in Section 4, we specifically demonstrate linearization of the integral equations and the Newton-type iterative method for solving inverse shape problem. Then some numerical examples are provided to demonstrate the effectiveness of the proposed linearized iterative scheme.

2 Problem formulation

Let $D \subset \mathbb{R}^2$ be an open and bounded domain, which is occupied by homogeneous and isotropic elastic medium with the density ρ . Assuming that the boundary ∂D be analytical and can be given as $\partial D = \Gamma_0 \cup \Gamma_m$, $\Gamma_0 \cap \Gamma_m = \emptyset$, where Γ_0 and Γ_m are the known part and the unknown part of the boundary ∂D . λ and μ , usually called Lemé constants, satisfy $\mu > 0$ and $\lambda + \mu > 0$. ω designates the frequency of vibration. The displacement field \mathbf{u} corresponding to the stress tensor $\boldsymbol{\sigma}(\mathbf{u})$ inside D satisfies the following Navier equation

$$\nabla \cdot \boldsymbol{\sigma}(\mathbf{u}) + \rho\omega^2\mathbf{u} = 0, \quad \text{in } D. \quad (2.1)$$

For a linear isotropic elastic medium, the components of the stress tensor $\boldsymbol{\sigma}(\mathbf{u})$ be

$$\boldsymbol{\sigma}_{ij} = \lambda\delta_{ij}\varepsilon_{\ell\ell} + 2\mu\varepsilon_{ij}, \quad i, j = 1, 2,$$

with the strain tensor ε_{ij} given by

$$\varepsilon_{ij} = \frac{1}{2} \left(\frac{\partial u_i}{\partial x_j} + \frac{\partial u_j}{\partial x_i} \right),$$

where δ_{ij} is the Kronecker delta function.

On the boundary ∂D , the displacement \mathbf{u} satisfies the following boundary conditions:

- Dirichlet boundary condition on Γ_0

$$\mathbf{u} = \mathbf{f}(\mathbf{x}, \omega), \quad \text{on } \Gamma_0. \quad (2.2)$$

- Impedance boundary condition on Γ_m

$$T_n \mathbf{u} + i\omega \chi \mathbf{u} = \mathbf{g}(\mathbf{x}, \omega), \quad \text{on } \Gamma_m. \quad (2.3)$$

The impedance function $\chi \geq 0$ is continuous.

For a fixed point $\mathbf{x} \in \partial D$, T the traction operator defined on the boundary ∂D , is given by

$$(T_n \mathbf{u})_\ell := \lambda n_\ell \frac{\partial u_j}{\partial x_j} + \mu n_j \left(\frac{\partial u_\ell}{\partial x_j} + \frac{\partial u_j}{\partial x_\ell} \right), \quad \ell = 1, 2,$$

where \mathbf{n} is the unit outward normal vector.

For a scalar function w , we have

$$\nabla w = \left(\frac{\partial w}{\partial x_1}, \frac{\partial w}{\partial x_2} \right)^\top, \quad \nabla^\perp w = \left(\frac{\partial w}{\partial x_2}, -\frac{\partial w}{\partial x_1} \right)^\top.$$

It is well-known that the displacement field \mathbf{u} can be splitted into the compressional and shear parts, i.e. the Helmholtz decomposition as following:

$$\mathbf{u} = \nabla u_p + \nabla^\perp u_s. \quad (2.4)$$

u_p and u_s , respectively, are the solutions of the following Helmholtz equations

$$\Delta u_p + \kappa_p^2 u_p = 0, \quad \Delta u_s + \kappa_s^2 u_s = 0.$$

κ_p and κ_s are the wave numbers of the compressional part and the shear part with the numbers $\kappa_p = \sqrt{\frac{\rho\omega^2}{\lambda+2\mu}}$ and $\kappa_s = \sqrt{\frac{\rho\omega^2}{\mu}}$.

Together with the equations (2.1) – (2.3) and (2.4), we get the problem considered as follows

$$\begin{cases} \Delta u_p + \kappa_p^2 u_p = 0, & \text{in } D, \\ \Delta u_s + \kappa_s^2 u_s = 0, & \text{in } D, \\ \mathbf{u} = \mathbf{f}(\mathbf{x}, \omega), & \text{on } \Gamma_0, \\ T_n \mathbf{u} + i\omega \chi \mathbf{u} = \mathbf{g}(\mathbf{x}, \omega), & \text{on } \Gamma_m. \end{cases} \quad (2.5)$$

Inverse Problem: The inverse problem we considered is to determine the shape of the unknown portion Γ_m and the impedance function χ from the displacement field $\mathbf{f}(\mathbf{x}, \omega)$ and the (measured) traction $\mathbf{t}(\mathbf{x}, \omega) = T_n \mathbf{u}$ on Γ_0 .

3 Numerical algorithm

We denote $\Phi(\kappa|\mathbf{x} - \mathbf{y}|)$ be the fundamental solution of the Helmholtz equation associated with the wavenumber κ , namely

$$\Phi(\kappa|\mathbf{x} - \mathbf{y}|) = \frac{i}{4} H_0^{(1)}(\kappa|\mathbf{x} - \mathbf{y}|), \quad (3.1)$$

with $H_0^{(1)}$ be the Hankel function of the first kind of order zero.

The displacement is $\mathbf{u} = \nabla u_p + \nabla^\perp u_s$. The vector components of the displacement \mathbf{u} will be

$$u_p(\mathbf{x}) = \int_{\partial B} \Phi(\kappa_p|\mathbf{x} - \mathbf{y}|) \varphi_1(\mathbf{y}) \mathrm{d}s(\mathbf{y}), \quad \mathbf{x} \in D, \quad (3.2)$$

and

$$u_s(\mathbf{x}) = \int_{\partial B} \Phi(\kappa_s|\mathbf{x} - \mathbf{y}|) \varphi_2(\mathbf{y}) \mathrm{d}s(\mathbf{y}), \quad \mathbf{x} \in D, \quad (3.3)$$

where φ_1, φ_2 are the density functions, $D \subset\subset B$, ∂B is the so called virtual boundary.

Combining (3.2), (3.3) and the definition of ∇^\perp for a scalar function, we have

$$\mathbf{u}(\mathbf{x}) = \int_{\partial B} \mathbb{E}(\mathbf{x}, \mathbf{y}) \varphi(\mathbf{y}) \mathrm{d}s(\mathbf{y}), \quad \mathbf{x} \in D, \quad (3.4)$$

with $\varphi = (\varphi_1, \varphi_2)^\top$ and

$$\mathbb{E}(\mathbf{x}, \mathbf{y}) = \begin{pmatrix} \frac{\partial \Phi(\kappa_p|\mathbf{x} - \mathbf{y}|)}{\partial x_1} & \frac{\partial \Phi(\kappa_s|\mathbf{x} - \mathbf{y}|)}{\partial x_2} \\ \frac{\partial \Phi(\kappa_p|\mathbf{x} - \mathbf{y}|)}{\partial x_2} & -\frac{\partial \Phi(\kappa_s|\mathbf{x} - \mathbf{y}|)}{\partial x_1} \end{pmatrix}.$$

Denote the unit outward normal vector by \mathbf{n} at $\mathbf{x} \in \partial D$, and the corresponding traction $T_n \mathbf{u}$ is given

$$(T_n \mathbf{u})(\mathbf{x}) = \int_{\partial B} \mathbb{T}(\mathbf{x}, \mathbf{y}) \varphi(\mathbf{y}) \mathrm{d}s(\mathbf{y}), \quad \mathbf{x} \in \partial D, \quad (3.5)$$

where the elements of the matrix \mathbb{T} are given by

$$\begin{aligned} \mathbb{T}_{1j}(\mathbf{x}, \mathbf{y}) &= \left[(\lambda + 2\mu) \frac{\partial \mathbb{E}_{1j}(\mathbf{x}, \mathbf{y})}{\partial x_1} + \lambda \frac{\partial \mathbb{E}_{2j}(\mathbf{x}, \mathbf{y})}{\partial x_2} \right] n_1 + \mu \left(\frac{\partial \mathbb{E}_{1j}(\mathbf{x}, \mathbf{y})}{\partial x_2} + \frac{\partial \mathbb{E}_{2j}(\mathbf{x}, \mathbf{y})}{\partial x_1} \right) n_2, \\ \mathbb{T}_{2j}(\mathbf{x}, \mathbf{y}) &= \mu \left(\frac{\partial \mathbb{E}_{1j}(\mathbf{x}, \mathbf{y})}{\partial x_2} + \frac{\partial \mathbb{E}_{2j}(\mathbf{x}, \mathbf{y})}{\partial x_1} \right) n_1 + \left[\lambda \frac{\partial \mathbb{E}_{1j}(\mathbf{x}, \mathbf{y})}{\partial x_1} + (\lambda + 2\mu) \frac{\partial \mathbb{E}_{2j}(\mathbf{x}, \mathbf{y})}{\partial x_2} \right] n_2, \\ j &= 1, 2. \end{aligned}$$

Denote by

$$\mathbf{S} \varphi(\mathbf{x}) := \int_{\partial B} \mathbb{E}(\mathbf{x}, \mathbf{y}) \varphi(\mathbf{y}) \mathrm{d}s(\mathbf{y}), \quad \mathbf{x} \in \mathbb{R}^2 \setminus \partial B, \quad (3.6)$$

and

$$\mathbf{K} \varphi(\mathbf{x}) := T_{n_x} \int_{\partial B} \mathbb{E}(\mathbf{x}, \mathbf{y}) \varphi(\mathbf{y}) \mathrm{d}s(\mathbf{y}). \quad (3.7)$$

Theorem 1. Define the operator $\mathbb{S}\varphi = \mathbf{S}\varphi|_{\partial D}$, then $\mathbb{S} : \mathbf{L}^2(\partial B) \rightarrow \mathbf{H}^{1/2}(\partial D)$ is compact, injective and dense range if $\rho\omega^2$ is not a Dirichlet eigenvalue of the negative lamé operator in the interior D .

Proof. It is easy to see that the kernel function of \mathbb{S} is analytic, we know that the operator $\mathbb{S} : \mathbf{L}^2(\partial B) \rightarrow \mathbf{H}^{1/2}(\partial D)$ is compact [6, Theorem 2.7]. Next, let $\mathbb{S}\varphi(\mathbf{x}) = 0$. Define

$$\mathbf{w}(\mathbf{x}) = \int_{\partial B} \mathbb{E}(\mathbf{x}, \mathbf{y})\varphi(\mathbf{y})ds(\mathbf{y}), \quad \mathbf{x} \in \mathbb{R}^2 \setminus \partial B, \quad (3.8)$$

then $\mathbf{w}(\mathbf{x})$ satisfies

$$\begin{cases} \mu\Delta\mathbf{w} + (\lambda + \mu)\nabla\nabla \cdot \mathbf{w} + \rho\omega^2\mathbf{w} = 0, & \text{in } D, \\ \mathbf{w}(\mathbf{x}) = \mathbf{0}, & \text{on } \partial D. \end{cases} \quad (3.9)$$

Since $\rho\omega^2$ is not a Dirichlet eigenvalue of the negative lamé operator in the interior D , which yields that $\mathbf{w}(\mathbf{x})$ vanishes in the inside of D . A unique continuation argument yields that $\mathbf{w}(\mathbf{x}) = 0$ in B . In fact, $\mathbf{w}(\mathbf{x})$ has the following form

$$\mathbf{w}(\mathbf{x}) = \nabla_{\mathbf{x}} \int_{\partial B} \Phi(\kappa_p|\mathbf{x} - \mathbf{y}|)\varphi_1(\mathbf{y})ds(\mathbf{y}) + \nabla_{\mathbf{x}}^\perp \int_{\partial B} \Phi(\kappa_s|\mathbf{x} - \mathbf{y}|)\varphi_2(\mathbf{y})ds(\mathbf{y}). \quad (3.10)$$

Denote

$$\phi(\mathbf{x}) = \int_{\partial B} \Phi(\kappa_p|\mathbf{x} - \mathbf{y}|)\varphi_1(\mathbf{y})ds(\mathbf{y}), \quad \mathbf{x} \in \mathbb{R}^2 \setminus \partial B,$$

and

$$\psi(\mathbf{x}) = \int_{\partial B} \Phi(\kappa_s|\mathbf{x} - \mathbf{y}|)\varphi_2(\mathbf{y})ds(\mathbf{y}), \quad \mathbf{x} \in \mathbb{R}^2 \setminus \partial B,$$

we have

$$\nabla\phi = -\nabla^\perp\psi, \quad \text{in } B. \quad (3.11)$$

Taking the dot product with ∇ and ∇^\perp , respectively, thus we have $\Delta\phi = 0$ and $\Delta\psi = 0$. Noting that ϕ and ψ satisfy the Helmholtz equations, we get $\phi = \psi = 0$ in B , and thus $\frac{\partial\phi_-}{\partial\nu} = \frac{\partial\psi_-}{\partial\nu} = 0$ on ∂B , where ν denotes the unit outward normal vector defined on ∂B and $-$ denotes the limits as $\mathbf{x} \rightarrow \partial B$ from inside of ∂B .

From the jump relation of the single-layer potential functions (see e.g. [6]), we can get

$$\phi_+ = \phi_-, \quad \text{and} \quad \frac{\partial\phi_-}{\partial\nu} - \frac{\partial\phi_+}{\partial\nu} = \varphi_1, \quad \text{on } \partial B, \quad (3.12)$$

where $+$ denotes the limits as $\mathbf{x} \rightarrow \partial B$ from outside of ∂B .

From equation (3.12), we know $\phi_+ = 0$ and $-\frac{\partial\phi_+}{\partial\nu} = \varphi_1$ on ∂B . This means that ϕ satisfies the homogeneous exterior Dirichlet boundary value problem with the

Sommerfeld radiation condition, the uniqueness for the exterior Dirichlet problem yields $\phi = 0$ outside of ∂B , and thus $\frac{\partial \phi^+}{\partial \nu} = 0$. Combining with equation (3.12), we have $\varphi_1 = 0$. The same argument will give $\varphi_2 = 0$. It means that the operator \mathbb{S} is injective with $\varphi = 0$.

Now we will show that \mathbb{S} has dense range in $\mathbf{H}^{1/2}(\partial D)$. Let $\psi \in \mathbf{H}^{-1/2}(\partial D)$ satisfy

$$\langle \mathbb{S}\varphi, \psi \rangle = 0, \quad \text{for } \varphi \in \mathbf{L}^2(\partial B), \quad (3.13)$$

It is sufficient to prove that $\psi = 0$.

$$\langle \mathbb{S}\varphi, \psi \rangle = \langle \varphi, \mathbb{S}^*\psi \rangle = 0, \quad (3.14)$$

which means

$$\begin{aligned} & \int_{\partial D} \overline{\psi}(\mathbf{x}) \cdot \int_{\partial B} \mathbb{E}(\mathbf{x}, \mathbf{y}) \varphi(\mathbf{y}) d\mathbf{s}(\mathbf{y}) d\mathbf{s}(\mathbf{x}) \\ &= \int_{\partial B} \varphi(\mathbf{y}) \cdot \int_{\partial D} \overline{\mathbb{E}^\top(\mathbf{x}, \mathbf{y})} \overline{\psi}(\mathbf{x}) d\mathbf{s}(\mathbf{x}) d\mathbf{s}(\mathbf{y}) \\ &= 0, \quad \text{for } \varphi \in \mathbf{L}^2(\partial B), \end{aligned} \quad (3.15)$$

we have

$$\int_{\partial D} \overline{\mathbb{E}^\top(\mathbf{x}, \mathbf{y})} \overline{\psi}(\mathbf{x}) d\mathbf{s}(\mathbf{x}) = 0, \quad \mathbf{y} \in \partial B. \quad (3.16)$$

Denote

$$\mathbf{w}'(\mathbf{y}) = \int_{\partial D} \mathbb{E}^\top(\mathbf{x}, \mathbf{y}) \psi(\mathbf{x}) d\mathbf{s}(\mathbf{x}), \quad \mathbf{y} \in \mathbb{R}^2 \setminus \partial D, \quad (3.17)$$

the component of $\mathbf{w}'(\mathbf{y})$ are

$$w'_1(\mathbf{y}) = \int_{\partial D} \left\{ \frac{\partial \Phi(\kappa_p |\mathbf{x} - \mathbf{y}|)}{\partial x_1} \psi_1(\mathbf{x}) + \frac{\partial \Phi(\kappa_p |\mathbf{x} - \mathbf{y}|)}{\partial x_2} \psi_2(\mathbf{x}) \right\} d\mathbf{s}(\mathbf{x}), \quad (3.18)$$

and

$$w'_2(\mathbf{y}) = \int_{\partial D} \left\{ \frac{\partial \Phi(\kappa_s |\mathbf{x} - \mathbf{y}|)}{\partial x_2} \psi_1(\mathbf{x}) - \frac{\partial \Phi(\kappa_s |\mathbf{x} - \mathbf{y}|)}{\partial x_1} \psi_2(\mathbf{x}) \right\} d\mathbf{s}(\mathbf{x}). \quad (3.19)$$

$w'_1(\mathbf{y})$ satisfies

$$\begin{cases} \Delta w'_1 + \kappa_p^2 w'_1 = 0, & \text{in } \mathbb{R}^2 \setminus \overline{B}, \\ w'_1(\mathbf{y}) = 0, & \text{on } \partial B. \end{cases} \quad (3.20)$$

and the Sommerfeld radiation condition. The uniqueness for the exterior Dirichlet problem yields $w'_1(\mathbf{y}) = 0$ outside of ∂B . A unique continuation argument yields that $w'_1(\mathbf{y}) = 0$ in $\mathbb{R}^2 \setminus \overline{D}$, thus also $w'_2(\mathbf{y}) = 0$ in $\mathbb{R}^2 \setminus \overline{D}$.

Denote

$$\tilde{\mathbf{w}}(\mathbf{y}) = \nabla w'_1(\mathbf{y}) + \nabla^\perp w'_2(\mathbf{y}), \quad \mathbf{y} \in \mathbb{R}^2 \setminus \partial D, \quad (3.21)$$

we have

$$\tilde{\mathbf{w}}(\mathbf{y})_+ = 0, \quad \text{and} \quad T_n \tilde{\mathbf{w}}(\mathbf{y})_+ = 0, \quad \text{on} \quad \partial D. \quad (3.22)$$

On the other hand, we have

$$\begin{aligned} \tilde{\mathbf{w}}(\mathbf{y}) &= \nabla_{\mathbf{y}} \int_{\partial D} \left\{ \frac{\partial \Phi(\kappa_p |\mathbf{x} - \mathbf{y}|)}{\partial x_1} \psi_1(\mathbf{x}) + \frac{\partial \Phi(\kappa_p |\mathbf{x} - \mathbf{y}|)}{\partial x_2} \psi_2(\mathbf{x}) \right\} \mathrm{d}s(\mathbf{x}) \\ &+ \nabla_{\mathbf{y}}^\perp \int_{\partial D} \left\{ \frac{\partial \Phi(\kappa_s |\mathbf{x} - \mathbf{y}|)}{\partial x_2} \psi_1(\mathbf{x}) - \frac{\partial \Phi(\kappa_s |\mathbf{x} - \mathbf{y}|)}{\partial x_1} \psi_2(\mathbf{x}) \right\} \mathrm{d}s(\mathbf{x}) \\ &= -\nabla_{\mathbf{y}} \int_{\partial D} \left\{ \frac{\partial \Phi(\kappa_p |\mathbf{x} - \mathbf{y}|)}{\partial y_1} \psi_1(\mathbf{x}) + \frac{\partial \Phi(\kappa_p |\mathbf{x} - \mathbf{y}|)}{\partial y_2} \psi_2(\mathbf{x}) \right\} \mathrm{d}s(\mathbf{x}) \\ &+ \nabla_{\mathbf{y}}^\perp \int_{\partial D} \left\{ -\frac{\partial \Phi(\kappa_s |\mathbf{x} - \mathbf{y}|)}{\partial y_2} \psi_1(\mathbf{x}) + \frac{\partial \Phi(\kappa_s |\mathbf{x} - \mathbf{y}|)}{\partial y_1} \psi_2(\mathbf{x}) \right\} \mathrm{d}s(\mathbf{x}) \\ &= \int_{\partial D} \Xi(\mathbf{x}, \mathbf{y}) \psi(\mathbf{x}) \mathrm{d}s(\mathbf{x}), \end{aligned}$$

with

$$\Xi(\mathbf{x}, \mathbf{y}) = - \begin{pmatrix} \frac{\partial^2 \Phi(\kappa_p |\mathbf{x} - \mathbf{y}|)}{\partial y_1^2} + \frac{\partial^2 \Phi(\kappa_s |\mathbf{x} - \mathbf{y}|)}{\partial y_2^2} & \frac{\partial^2 (\Phi(\kappa_p |\mathbf{x} - \mathbf{y}|) - \Phi(\kappa_s |\mathbf{x} - \mathbf{y}|))}{\partial y_2 \partial y_1} \\ \frac{\partial^2 (\Phi(\kappa_p |\mathbf{x} - \mathbf{y}|) - \Phi(\kappa_s |\mathbf{x} - \mathbf{y}|))}{\partial y_1 \partial y_2} & \frac{\partial^2 \Phi(\kappa_p |\mathbf{x} - \mathbf{y}|)}{\partial y_2^2} + \frac{\partial^2 \Phi(\kappa_s |\mathbf{x} - \mathbf{y}|)}{\partial y_1^2} \end{pmatrix}.$$

Since $\Phi(\kappa_p |\mathbf{x} - \mathbf{y}|)$ and $\Phi(\kappa_s |\mathbf{x} - \mathbf{y}|)$ satisfy the Helmholtz equations, with a simple calculation, we have

$$\begin{aligned} \Xi(\mathbf{x}, \mathbf{y}) &= - \begin{pmatrix} \frac{\partial^2 \Phi(\kappa_p |\mathbf{x} - \mathbf{y}|)}{\partial y_1^2} + \frac{\partial^2 \Phi(\kappa_s |\mathbf{x} - \mathbf{y}|)}{\partial y_2^2} & \frac{\partial^2 (\Phi(\kappa_p |\mathbf{x} - \mathbf{y}|) - \Phi(\kappa_s |\mathbf{x} - \mathbf{y}|))}{\partial y_2 \partial y_1} \\ \frac{\partial^2 (\Phi(\kappa_p |\mathbf{x} - \mathbf{y}|) - \Phi(\kappa_s |\mathbf{x} - \mathbf{y}|))}{\partial y_1 \partial y_2} & \frac{\partial^2 \Phi(\kappa_p |\mathbf{x} - \mathbf{y}|)}{\partial y_2^2} + \frac{\partial^2 \Phi(\kappa_s |\mathbf{x} - \mathbf{y}|)}{\partial y_1^2} \end{pmatrix}, \\ &= \kappa_s^2 \Phi(\kappa_s |\mathbf{x} - \mathbf{y}|) \mathbf{I} + \nabla \nabla^\top (\Phi(\kappa_s |\mathbf{x} - \mathbf{y}|) - \Phi(\kappa_p |\mathbf{x} - \mathbf{y}|)), \\ &= \rho \omega^2 \Gamma(\mathbf{x}, \mathbf{y}), \end{aligned}$$

where $\Gamma(\mathbf{x}, \mathbf{y})$ is the fundamental matrix (see e.g. [18, 30]), and \mathbf{I} is the identity matrix.

From the jump relation of the single-layer potential functions (see e.g. [15, 23, 30]), we can get

$$\tilde{\mathbf{w}}(\mathbf{y})_+ = \tilde{\mathbf{w}}(\mathbf{y})_-, \quad \text{on} \quad \partial D, \quad (3.23)$$

and

$$T_n \tilde{\mathbf{w}}(\mathbf{y})_- - T_n \tilde{\mathbf{w}}(\mathbf{y})_+ = \omega^2 \psi, \quad \text{on} \quad \partial D. \quad (3.24)$$

Thus, by the equation (3.22), we have $\tilde{\mathbf{w}}(\mathbf{y})_- = 0$, which yields that $\tilde{\mathbf{w}}(\mathbf{y})$ satisfy the Navier equation with homogeneous Dirichlet boundary value in D . Since $\rho\omega^2$ is not a Dirichlet eigenvalue of the negative lamé operator in the interior D , which yields that $\tilde{\mathbf{w}}(\mathbf{y})$ vanishes in the inside of D thus also $T_n\tilde{\mathbf{w}}(\mathbf{y})_- = 0$. From the equation (3.24), we have $\psi = 0$, which completes the proof. \square

On Γ_0 , define the operator \mathcal{N} by

$$\mathcal{N}\varphi(\mathbf{x}) := \begin{pmatrix} \mathbf{S}\varphi(\mathbf{x})|_{\Gamma_0} \\ T_{n_x}\mathbf{S}\varphi(\mathbf{x})|_{\Gamma_0} \end{pmatrix}, \quad \mathbf{x} \in \Gamma_0.$$

Theorem 2. *The operator $\mathcal{N} : \mathbf{L}^2(\partial B) \rightarrow \mathbf{H}^{1/2}(\Gamma_0) \times \mathbf{H}^{-1/2}(\Gamma_0)$ is compact and injective.*

Proof. The operator $\mathcal{N} : \mathbf{L}^2(\partial B) \rightarrow \mathbf{H}^{1/2}(\Gamma_0) \times \mathbf{H}^{-1/2}(\Gamma_0)$ is compact by the kernel function of \mathcal{N} being analytic [6, Theorem 2.7]. If we let $\mathcal{N}\varphi = 0$, it should be injective by $\varphi = 0$. The uniqueness of the Cauchy problem yields that $\mathbf{S}\varphi = 0$ in D . The same argument from Theorem 1 will give $\varphi = 0$. Therefore the operator \mathcal{N} is injective. \square

After this, we write the problem considered in this paper. First, we approximate the solution \mathbf{u} of equation (2.1). In this step, we should find the density function $\varphi \in \mathbf{L}^2(\partial B)$ by

$$\mathcal{N}\varphi = \mathbf{h}, \quad (3.25)$$

here $\mathbf{h} = (\mathbf{f}|_{\Gamma_0}, \mathbf{t}|_{\Gamma_0})^\top$, and then $\mathbf{S}\varphi(\mathbf{x})$ will approximate the displacement \mathbf{u} in D . Second, a Newton type method is used to recover the missing boundary Γ_m and the impedance function χ .

Before giving the uniqueness result, we should first give a property of the solution $\mathbf{u}(\mathbf{x}, \omega)$.

Lemma 3.1. *The displacement $\mathbf{u}(\mathbf{x}, \omega)$ depends analytically on $\omega \in \mathbb{C}$, if $\mathbf{h}(\mathbf{x}, \omega)$ depends analytically on $\omega \in \mathbb{C}$.*

Proof. We seek the displacement field in the form as

$$\mathbf{u}(\mathbf{x}) = \int_{\partial B} \mathbb{E}(\mathbf{x}, \mathbf{y})\varphi(\mathbf{y})d\mathbf{s}(\mathbf{y}), \quad \mathbf{x} \in D, \quad (3.26)$$

with $\varphi = (\varphi_1, \varphi_2)^\top$ and

$$\mathbb{E}(\mathbf{x}, \mathbf{y}) = \begin{pmatrix} \frac{\partial\Phi(\kappa_p|\mathbf{x}-\mathbf{y}|)}{\partial x_1} & \frac{\partial\Phi(\kappa_s|\mathbf{x}-\mathbf{y}|)}{\partial x_2} \\ \frac{\partial\Phi(\kappa_p|\mathbf{x}-\mathbf{y}|)}{\partial x_2} & -\frac{\partial\Phi(\kappa_s|\mathbf{x}-\mathbf{y}|)}{\partial x_1} \end{pmatrix}.$$

Since the fundamental solution to the Helmholtz equation depends analytically on wavenumber κ_p or κ_s [6], and thus it depends analytically on ω . From $\mathcal{N}\varphi = \mathbf{h}$ and $\mathbf{h}(\mathbf{x}, \omega)$ depends analytically on $\omega \in \mathbb{C}$, we know that φ depends analytically on $\omega \in \mathbb{C}$. From the above representation (3.26), it can be seen that the displacement field $\mathbf{u}(\mathbf{x}, \omega)$ depends analytically on ω . \square

In the end of this section, we state a uniqueness theorem for the inverse problem under the assumption that we have the knowledge of the Cauchy data pair.

Theorem 3. *Assume that D_1 and D_2 are elastic bodies with impedance χ_1 and χ_2 , respectively, $\partial D_1 \cap \partial D_2 = \Gamma_0$. The corresponding displacements $\mathbf{u}_1(\mathbf{x}, \omega)$, $\mathbf{u}_2(\mathbf{x}, \omega)$ satisfy*

$$\mathbf{u}_1(\mathbf{x}, \omega)|_{\Gamma_0} = \mathbf{u}_2(\mathbf{x}, \omega)|_{\Gamma_0}, \quad T_n \mathbf{u}_1(\mathbf{x}, \omega)|_{\Gamma_0} = T_n \mathbf{u}_2(\mathbf{x}, \omega)|_{\Gamma_0}$$

for the frequency $\omega \in (a, b)$. Then $D_1 = D_2$ and $\chi_1 = \chi_2$.

Proof. Assume that there are two different domains D_1, D_2 with the boundary coefficients χ_1 and χ_2 generating the same Cauchy data pair denoted by (\mathbf{f}, \mathbf{t}) on Γ_0 , $\Gamma_m^{(j)} = \partial D_j \setminus \Gamma_0$. Let $\mathbf{u}_j(\mathbf{x}, \omega), j = 1, 2$ be the solutions

$$\begin{cases} \nabla \cdot \boldsymbol{\sigma}(\mathbf{u}_j) + \rho\omega^2 \mathbf{u}_j = 0, & \text{in } D_j, \\ \mathbf{u}_j = \mathbf{f}(\mathbf{x}, \omega), & \text{on } \Gamma_0, \\ T_{n_j} \mathbf{u}_j + i\omega_j \chi_j \mathbf{u}_j = 0, & \text{on } \Gamma_m^{(j)}. \end{cases} \quad (3.27)$$

First, we prove $\Gamma_m^{(1)} = \Gamma_m^{(2)}$. It should be noted that $\mathbf{f}(\mathbf{x}, \omega) \neq 0$. Assume on the contradiction that $\Gamma_m^{(1)} \neq \Gamma_m^{(2)}$. Without loss of generality we suppose that there is a point in $D_1 \setminus \overline{D_2}$. Otherwise we may switch the notations D_1 and D_2 if necessary. Then we can always find a domain $D^* \subset D_1$ such that $\partial D^* = \Lambda_1 \cup \Lambda_2$, $\Lambda_1 \subset \Gamma_m^{(1)}$, $\Lambda_2 \subset \Gamma_m^{(2)}$, $\Lambda_2 \in (\overline{D_1} \cap \overline{D_2})$.

On Λ_1 , we have

$$T_{n_1} \mathbf{u}_1(\mathbf{x}, \omega) = -i\omega \chi_1 \mathbf{u}_1(\mathbf{x}, \omega). \quad (3.28)$$

On Λ_2 , we have

$$T_{n_2} \mathbf{u}_2(\mathbf{x}, \omega) = -i\omega \chi_2 \mathbf{u}_2(\mathbf{x}, \omega). \quad (3.29)$$

Since $\mathbf{u}_1(\mathbf{x}, \omega) = \mathbf{u}_2(\mathbf{x}, \omega)$ on Γ_0 , the uniqueness of the Cauchy problem for elliptic equations will give $\mathbf{u}_1(\mathbf{x}, \omega) = \mathbf{u}_2(\mathbf{x}, \omega)$ in D^* . By $\Lambda_2 \in (\overline{D_1} \cap \overline{D_2})$, we get $\mathbf{u}_1(\mathbf{x}, \omega) = \mathbf{u}_2(\mathbf{x}, \omega)$, and then

$$T_{n_2} \mathbf{u}_1(\mathbf{x}, \omega) = -i\omega \chi_2 \mathbf{u}_1(\mathbf{x}, \omega). \quad (3.30)$$

Let $\boldsymbol{\nu} = -\mathbf{n}_2, \chi = -\chi_2$ on Λ_2 and $\boldsymbol{\nu} = \mathbf{n}_1, \chi = \chi_1$ on Λ_1 , combining equations (3.28) and (3.30), we have

$$T_{\boldsymbol{\nu}} \mathbf{u}_1(\mathbf{x}, \omega) = -i\omega \chi \mathbf{u}_1(\mathbf{x}, \omega), \quad \text{on } \partial D^*. \quad (3.31)$$

Since $D^* \subset \overline{D_1}$, we know that $\mathbf{u}_1(\mathbf{x}, \omega)$ satisfy the Navier equation in D^* with the boundary condition (3.31). The first Betti formula yields

$$\int_{D^*} (E(\mathbf{u}_1, \overline{\mathbf{u}}_1) - \rho\omega^2 |\mathbf{u}_1(\mathbf{x}, \omega)|^2) dx = \int_{\partial D^*} T_{\boldsymbol{\nu}} \mathbf{u}_1(\mathbf{x}, \omega) \cdot \overline{\mathbf{u}}_1(\mathbf{x}, \omega) ds,$$

where

$$\begin{aligned}
E(\mathbf{u}_1, \bar{\mathbf{u}}_1) &= \nabla \mathbf{u}_1(\mathbf{x}, \omega) : \mathcal{C} : \nabla \bar{\mathbf{u}}_1(\mathbf{x}, \omega) \\
&= \lambda \operatorname{div} \mathbf{u}_1 \operatorname{div} \bar{\mathbf{u}}_1 + \mu \sum_{p,q=1}^2 \frac{\partial u_p}{\partial x_q} \left(\overline{\frac{\partial u_p}{\partial x_q}} + \frac{\partial u_q}{\partial x_p} \right) \\
&= \lambda |\operatorname{div} \mathbf{u}_1|^2 + 2\mu \left(\left| \frac{\partial u_1}{\partial x_1} \right|^2 + \left| \frac{\partial u_2}{\partial x_2} \right|^2 \right) + \mu \left(\left| \frac{\partial u_1}{\partial x_2} + \frac{\partial u_2}{\partial x_1} \right|^2 \right).
\end{aligned} \tag{3.32}$$

Combining the boundary condition (3.31), we have

$$\int_{D^*} (E(\mathbf{u}_1, \bar{\mathbf{u}}_1) - \rho \omega^2 |\mathbf{u}_1(\mathbf{x}, \omega)|^2) dx + i\omega \chi \int_{\partial D^*} |\mathbf{u}_1(\mathbf{x}, \omega)|^2 ds = 0.$$

Taking the real part in the above equation, we have

$$\int_{D^*} (E(\mathbf{u}_1, \bar{\mathbf{u}}_1) - \rho \omega^2 |\mathbf{u}_1(\mathbf{x}, \omega)|^2) dx = 0, \quad \text{for all } \omega \in (a, b). \tag{3.33}$$

The analytical dependance of $u_1(\mathbf{x}, \omega)$ on ω implies that equation (3.33) is valid for $\omega \in \mathbb{C}$.

Now choosing $\omega = 1 + i\delta$ we get $\omega^2 = 1 - \delta^2 + 2i\delta$, then the equation (3.33) will be

$$\int_{D^*} (E(\mathbf{u}_1, \bar{\mathbf{u}}_1) - \rho(1 - \delta^2) |\mathbf{u}_1(\mathbf{x}, \omega)|^2) dx + 2i\rho\delta \int_{D^*} |\mathbf{u}_1(\mathbf{x}, \omega)|^2 dx = 0, \tag{3.34}$$

which implies

$$\rho\delta \int_{D^*} |\mathbf{u}_1(\mathbf{x}, \omega)|^2 dx = 0, \quad \text{for all } \omega = 1 + i\delta, \delta \in \mathbb{R} \tag{3.35}$$

by taking the imaginary part of the equation (3.34). Again using the analytical dependance, we get

$$\mathbf{u}_1(\mathbf{x}, \omega) = 0, \quad \text{in } D^* \tag{3.36}$$

for all $\omega \in \mathbb{C}$. By the uniqueness of the analytic continuation, thus $\mathbf{u}_1(\mathbf{x}, \omega) = 0$ in D_1 for all $\omega \in \mathbb{C}$. This yields

$$\mathbf{f}(\mathbf{x}, \omega) = \mathbf{u}_1(\mathbf{x}, \omega)|_{\Gamma_0} = 0,$$

which contradicts the fact that $\mathbf{f}(\mathbf{x}, \omega) \neq 0$. Hence $\Gamma_m^{(1)} = \Gamma_m^{(2)} = \Gamma_m$, i.e. $D_1 = D_2 = D$.

Next we will check $\chi_1 = \chi_2$. On Γ_0 , we have

$$\mathbf{u}_1(\mathbf{x}, \omega) = \mathbf{u}_2(\mathbf{x}, \omega)$$

and

$$T_n \mathbf{u}_1(\mathbf{x}, \omega) = T_n \mathbf{u}_2(\mathbf{x}, \omega),$$

the uniqueness of the Cauchy problem for elliptic equations will give

$$\mathbf{u}_1(\mathbf{x}, \omega) = \mathbf{u}_2(\mathbf{x}, \omega), \quad \text{in } D. \quad (3.37)$$

Together with $T_n \mathbf{u}_1(\mathbf{x}, \omega) = -i\omega \chi_1 \mathbf{u}_1(\mathbf{x}, \omega)$ and $T_n \mathbf{u}_2(\mathbf{x}, \omega) = -i\omega \chi_2 \mathbf{u}_2(\mathbf{x}, \omega)$ on Γ_m , we have $i\omega \chi_1 \mathbf{u}_1(\mathbf{x}, \omega) = i\omega \chi_2 \mathbf{u}_1(\mathbf{x}, \omega)$, i.e. $i\omega(\chi_1 - \chi_2) \mathbf{u}_1(\mathbf{x}, \omega) = 0$ on Γ_m . If $\mathbf{u}_1(\mathbf{x}, \omega) = 0$ on any open subset $\Gamma \subset \Gamma_m$, we have $T_n \mathbf{u}_1(\mathbf{x}, \omega) = -i\omega \chi_1 \mathbf{u}_1(\mathbf{x}, \omega) = 0$ on Γ . The uniqueness of the Cauchy problem for elliptic equations will give $\mathbf{u}_1(\mathbf{x}, \omega) \equiv 0$ in D . This is a contradiction to the behavior of $\mathbf{u}_1(\mathbf{x}, \omega)$ on Γ_0 with $\mathbf{f}(\mathbf{x}, \omega) \neq 0$. Thus we have $\chi_1 - \chi_2 = 0$ on Γ_m . The proof is completed. \square

4 Recovery method

As discussing in the previous section, we should solve a Cauchy problem first.

4.1 The Cauchy problem

In order to solve the Cauchy problem, we should consider the perturbed equations

$$\mathcal{N} \boldsymbol{\varphi}^\delta = \mathbf{h}^\delta. \quad (4.1)$$

Here, $\mathbf{h}^\delta = (\mathbf{f}^\delta, \mathbf{t}^\delta)^\top \in L^2(\Gamma_0) \times L^2(\Gamma_0)$ is measured noisy data satisfying

$$\|\mathbf{h}^\delta - \mathbf{h}\| \leq \delta \times \|\mathbf{h}\| := \epsilon,$$

where δ is the noise level.

The minimum norm solution (see e.g. [21]) of (3.25) is to solve the following equation

$$\alpha \boldsymbol{\varphi}_\alpha^\delta + \mathcal{N}^* \mathcal{N} \boldsymbol{\varphi}_\alpha^\delta = \mathcal{N}^* \mathbf{h}^\delta, \quad \alpha > 0.$$

and choosing the regularization parameter by Morozov discrepancy principle, i.e. via finding the zero of $G(\alpha) := \|\mathcal{N} \boldsymbol{\varphi}_\alpha^\delta - \mathbf{h}^\delta\|^2 - \epsilon^2$. The regularization parameter will be obtained numerically by Newton's method as following:

1. Set $n = 0$, and give an initial regularization parameter $\alpha_0 > 0$.
2. Get $\boldsymbol{\varphi}_{\alpha_n}^\delta$ from $(\alpha_n I + \mathcal{N}^* \mathcal{N}) \boldsymbol{\varphi}_{\alpha_n}^\delta = \mathcal{N}^* \mathbf{h}^\delta$.
3. Get $\frac{d}{d\alpha} \boldsymbol{\varphi}_{\alpha_n}^\delta$ from $(\alpha_n I + \mathcal{N}^* \mathcal{N}) \frac{d}{d\alpha} \boldsymbol{\varphi}_{\alpha_n}^\delta = -\boldsymbol{\varphi}_{\alpha_n}^\delta$.
4. Get $F(\alpha_n)$ and $F'(\alpha_n)$ by

$$F(\alpha_n) = \|\mathcal{N} \boldsymbol{\varphi}_{\alpha_n}^\delta - \mathbf{h}^\delta\|^2 - \epsilon^2$$

and

$$F'(\alpha_n) = 2\alpha_n \left\| \mathcal{N} \frac{d}{d\alpha} \varphi_{\alpha_n}^\delta \right\|^2 + 2\alpha_n^2 \left\| \frac{d}{d\alpha} \varphi_{\alpha_n}^\delta \right\|^2,$$

respectively.

5. Set $\alpha_{n+1} = \alpha_n - \frac{F(\alpha_n)}{F'(\alpha_n)}$. If $|\alpha_{n+1} - \alpha_n| < \varepsilon$ ($\varepsilon \ll 1$), end. Else, set $n = n + 1$ return to 2.

If the regularization parameter is fixed by α^* , we can achieve the regularized solution $\varphi_{\alpha^*}^\delta = R_\alpha \mathbf{h}^\delta$ by introducing the regularization operator

$$R_{\alpha^*} := (\alpha^* I + \mathcal{N}^* \mathcal{N})^{-1} \mathcal{N}^*.$$

The displacement \mathbf{u} can be given by $\mathbf{u}(\mathbf{x}) \approx \mathbf{S} \varphi_{\alpha^*}^\delta(\mathbf{x})$, which is treated data in the iterative method.

4.2 Newton-type method

In the above section, we have given the approximation of the displacement \mathbf{u} in B by solving equation (3.25), namely $\mathbf{S} \varphi(\mathbf{x})$. Then we can get the gradient explicitly. In the two dimensional case, the gradient of the approximate the displacement $\mathbf{S} \varphi(\mathbf{x})$ can be calculated by

$$\nabla \mathbf{S} \varphi(\mathbf{x}) = \int_{\partial B} (\nabla \nabla^\top \Phi(\kappa_p |\mathbf{x} - \mathbf{y}|) \varphi_1(\mathbf{y}) + \nabla \nabla^\perp \Phi(\kappa_s |\mathbf{x} - \mathbf{y}|) \varphi_2(\mathbf{y})) d\mathbf{s}(\mathbf{y}). \quad (4.2)$$

Based on the gradient of the approximate scattered field, we are now ready to propose the Newton-type iteration scheme for recovering ∂D .

For the sake of simplicity, we assume that the boundary is starlike with respect to the origin, i.e. ∂D can be represented in the parametric form

$$\partial D = \{r(\vartheta)(\cos \vartheta, \sin \vartheta), \vartheta \in [0, 2\pi)\}$$

where $r : R \rightarrow R$ is a positive, twice continuously differentiable and 2π -periodic function. In this paper we assume that

$$\Gamma_0 = \{r(\vartheta)(\cos \vartheta, \sin \vartheta), \vartheta \in [0, \pi)\}$$

as the known part coincides with the measured Cauchy data and

$$\Gamma_m = \{r(\vartheta)(\cos \vartheta, \sin \vartheta), \vartheta \in [\pi, 2\pi)\}$$

as the missing part of the boundary with the absorbing boundary condition.

To numerically approximate $r(\vartheta)$, we assume that $r(\vartheta)$ is represented as the trigonometric polynomials of degree less than or equal to N , namely

$$r(\vartheta) = a_0 + \sum_{j=1}^N (a_j \cos j\vartheta + b_j \sin j\vartheta). \quad (4.3)$$

Our reconstruction algorithm can be summarized as follows:

First, for a given Cauchy data pair (\mathbf{f}, \mathbf{t}) on Γ_0 , we can get the density function φ by

$$\mathcal{N}\varphi(\mathbf{x}) = \mathbf{h}, \quad \mathbf{x} \in \Gamma_0. \quad (4.4)$$

Then we can get the treated data $\mathbf{S}\varphi(\mathbf{x})$ for a given function \mathbf{g} .

Second, for the current approximation to the missing boundary curve r and the impedance χ we compute $\mathcal{M}_D\varphi = \mathbf{S}\varphi(\mathbf{x})|_{\Gamma_m}$ and $\mathcal{M}_T\varphi = T_n\mathbf{S}\varphi(\mathbf{x})|_{\Gamma_m}$. Denote $\mathcal{F} = \mathcal{M}_T + i\omega\chi\mathcal{M}_D$ be the combination.

Third, obtain the update Δr and $\Delta\chi$ for the boundary parameterization and the impedance by

$$\mathcal{F}(r, \chi) + d\mathcal{F}(r, \chi; \Delta r, \Delta\chi) = \mathbf{g}, \quad (4.5)$$

the above equation can be written as

$$T_n\mathbf{S}\varphi + dT_n\mathbf{S}\varphi + i\omega\chi(\mathbf{S}\varphi + d\mathbf{S}\varphi) + i\omega d\chi\mathbf{S}\varphi = \mathbf{g},$$

once we have gotten Δr and $\Delta\chi$ we can update r and χ by replacing r by $r + \Delta r$ and χ by $\chi + \Delta\chi$.

Remark 4.1. *In the third step, we will deal this by a two step Newton iterative method. We get the update Δr for the boundary parameterization by*

$$T_n\mathbf{S}\varphi + dT_n\mathbf{S}\varphi + i\omega\chi(\mathbf{S}\varphi + d\mathbf{S}\varphi) = \mathbf{g}. \quad (4.6)$$

Then we will, for the boundary parameterization $r + \Delta r$, get the update $\Delta\chi$ for the impedance function by

$$T_n\mathbf{S}\varphi + i\omega\chi\mathbf{S}\varphi + i\omega d\chi\mathbf{S}\varphi = \mathbf{g}. \quad (4.7)$$

The Fréchet derivatives of the integral operators \mathbf{S} and $T_n\mathbf{S}$ with respect to \mathbf{x} can be calculated by

$$d\mathbf{S}\varphi = \nabla \mathbf{u} = \begin{pmatrix} \partial_{x_1}u_1 & \partial_{x_2}u_1 \\ \partial_{x_1}u_2 & \partial_{x_2}u_2 \end{pmatrix},$$

$$dT_n\mathbf{S}\mathbf{g} = \nabla T_n\mathbf{u} = \begin{pmatrix} \partial_{x_1}(T_n\mathbf{u})_1 & \partial_{x_2}(T_n\mathbf{u})_1 \\ \partial_{x_1}(T_n\mathbf{u})_2 & \partial_{x_2}(T_n\mathbf{u})_2 \end{pmatrix},$$

where

$$\begin{aligned} \partial_{x_1}u_1 &= \int_{\partial B} \partial_{x_1}\mathbb{E}_{11}g_1(\mathbf{y}) + \partial_{x_1}\mathbb{E}_{12}g_2(\mathbf{y})ds(\mathbf{y}), \\ \partial_{x_2}u_1 &= \int_{\partial B} \partial_{x_2}\mathbb{E}_{11}g_1(\mathbf{y}) + \partial_{x_2}\mathbb{E}_{12}g_2(\mathbf{y})ds(\mathbf{y}), \\ \partial_{x_1}u_2 &= \int_{\partial B} \partial_{x_1}\mathbb{E}_{21}g_1(\mathbf{y}) + \partial_{x_1}\mathbb{E}_{22}g_2(\mathbf{y})ds(\mathbf{y}), \\ \partial_{x_2}u_2 &= \int_{\partial B} \partial_{x_2}\mathbb{E}_{21}g_1(\mathbf{y}) + \partial_{x_2}\mathbb{E}_{22}g_2(\mathbf{y})ds(\mathbf{y}), \end{aligned}$$

$$\begin{aligned}
\partial_{x_1}(T_n \mathbf{u})_1 &= \int_{\partial B} \partial_{x_1} \mathbb{T}_{11} g_1(\mathbf{y}) + \partial_{x_1} \mathbb{T}_{12} g_2(\mathbf{y}) ds(\mathbf{y}), \\
\partial_{x_2}(T_n \mathbf{u})_1 &= \int_{\partial B} \partial_{x_2} \mathbb{T}_{11} g_1(\mathbf{y}) + \partial_{x_2} \mathbb{T}_{12} g_2(\mathbf{y}) ds(\mathbf{y}), \\
\partial_{x_1}(T_n \mathbf{u})_2 &= \int_{\partial B} \partial_{x_1} \mathbb{T}_{21} g_1(\mathbf{y}) + \partial_{x_1} \mathbb{T}_{22} g_2(\mathbf{y}) ds(\mathbf{y}), \\
\partial_{x_2}(T_n \mathbf{u})_2 &= \int_{\partial B} \partial_{x_2} \mathbb{T}_{21} g_1(\mathbf{y}) + \partial_{x_2} \mathbb{T}_{22} g_2(\mathbf{y}) ds(\mathbf{y}), \\
\partial_{\mathbf{x}} \mathbb{E}(\mathbf{x}, \mathbf{y}) &= \begin{pmatrix} \partial_{x_1} \mathbb{E}_{11} + \partial_{x_2} \mathbb{E}_{11} & \partial_{x_1} \mathbb{E}_{12} + \partial_{x_2} \mathbb{E}_{12} \\ \partial_{x_1} \mathbb{E}_{21} + \partial_{x_2} \mathbb{E}_{21} & \partial_{x_1} \mathbb{E}_{22} + \partial_{x_2} \mathbb{E}_{22} \end{pmatrix}, \\
\partial_{\mathbf{x}} \mathbf{T}_n \mathbb{E}(\mathbf{x}, \mathbf{y}) &= \begin{pmatrix} \partial_{x_1} \mathbb{T}_{11} + \partial_{x_2} \mathbb{T}_{11} & \partial_{x_1} \mathbb{T}_{12} + \partial_{x_2} \mathbb{T}_{12} \\ \partial_{x_1} \mathbb{T}_{21} + \partial_{x_2} \mathbb{T}_{21} & \partial_{x_1} \mathbb{T}_{22} + \partial_{x_2} \mathbb{T}_{22} \end{pmatrix}.
\end{aligned}$$

For this iterative algorithm, we have to create a stopping criterion. For convenience, the stopping of the iterative process we perform with the following relative error

$$E_n = \frac{\|\Delta r_n\|_{L^2}}{\|r_{n-1}\|_{L^2}} + \frac{\|\Delta \chi_n\|_{L^2}}{\|\chi_{n-1}\|_{L^2}}. \quad (4.8)$$

We choose a constant $\varepsilon > 0$. If $E_n > \varepsilon$, the iteration process is continued. Otherwise, it is stopped.

5 Numerical Examples

In this part, we will give some examples to show the effectiveness of the present method. The Lemé constants λ and μ are given by $\lambda = 1$ and $\mu = 1$. The inside of the elastic obstacle is assumed to be filled with a homogeneous and isotropic elastic medium with a unit mass, i.e. $\rho = 1$. The wavenumbers κ_p and κ_s are usually determined by the relationship between the wavenumbers and the Lemé constants $\kappa_p = \sqrt{\frac{\rho\omega^2}{\lambda+2\mu}}$ and $\kappa_s = \sqrt{\frac{\rho\omega^2}{\mu}}$. The initial guess of the boundary is a half circle, and the initial guess of the impendence function is a constant function. The number of the coefficients is 17, i.e. $N = 8$ in equation (4.3).

In the practice, we known all the information of the known part including the Cauchy data pair (\mathbf{f}, \mathbf{t}) about Γ_0 . And we can easily get the equation $T_n \mathbf{u} + i\omega \chi \mathbf{u} = \mathbf{g}$ on Γ_0 . Thus we can deal with iterative procedure on the whole boundary ∂D . The initial guess of the boundary is a circle. The results about the known part can give a reference result for the present method.

Example 5.1. *In this example, D is a apple-shaped domain, and the boundary ∂D be*

$$\mathbf{z}(\vartheta) = \frac{1 + 0.8 \cos \vartheta + 0.2 \sin 2\vartheta}{1 + 0.7 \cos \vartheta} (\cos \vartheta, \sin \vartheta)$$

with the parameterized surface impedance χ given by $\chi(\vartheta) = \sin^4 \vartheta, \vartheta \in [\pi, 2\pi]$. The components u_p and u_s of the displacement \mathbf{u} inside the elastic obstacle are generated by

$$u_p(\mathbf{x}) = J_0^{(1)}(\kappa_p |\mathbf{x} - \mathbf{y}_0|), \quad u_s(\mathbf{x}) = J_0^{(1)}(\kappa_s |\mathbf{x} - \mathbf{y}_0|), \quad \mathbf{x} \in \overline{D},$$

where $\mathbf{y}_0 = (1, 0)$, i.e. $\mathbf{u}(\mathbf{x}) = \nabla u_p(\mathbf{x}) + \nabla^\perp u_s(\mathbf{x})$. We fix the frequency by $\omega = 3$. The so called virtual boundary ∂B is a circle, and its radius is 4. The initial guess of the boundary is a circle, and its radius is 0.3. Figure 1 shows the numerical reconstructions of the missing boundary and the impedance function with different noise levels $\delta \in \{0\%, 1\%, 5\%\}$ for Example 5.1. We can see that the numerical reconstructions are satisfactory. The reconstruction improves as the noise decreases.

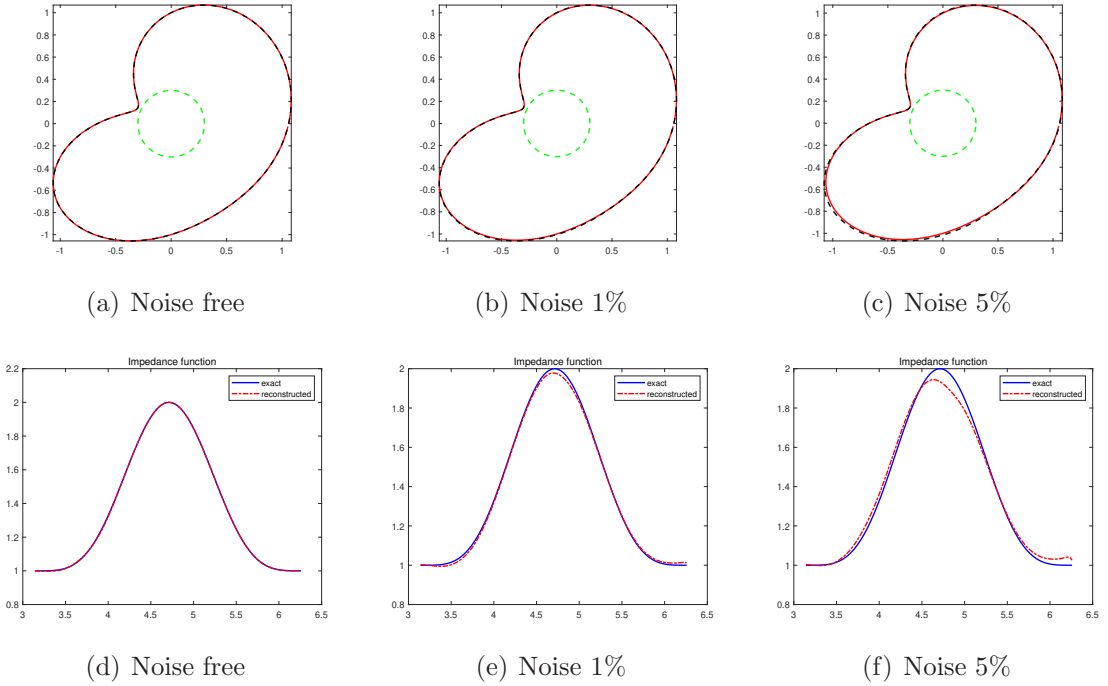


Figure 1: The numerical reconstructions of the shape and the impedance function χ with different noise levels $\delta \in \{0\%, 1\%, 5\%\}$ in Example 5.1.

Example 5.2. The components u_p and u_s of the displacement \mathbf{u} inside the elastic obstacle are generated by

$$u_p(\mathbf{x}) = \frac{i}{4} H_0^{(1)}(\kappa_p |\mathbf{x} - \mathbf{y}_0|), \quad u_s(\mathbf{x}) = \frac{i}{4} H_0^{(1)}(\kappa_s |\mathbf{x} - \mathbf{y}_0|), \quad \mathbf{x} \in \overline{D},$$

i.e. $\mathbf{u}(\mathbf{x}) = \nabla u_p(\mathbf{x}) + \nabla^\perp u_s(\mathbf{x})$. The so called virtual boundary ∂B is a circle, and its radius is 4. The initial guess of the boundary is a circle as in Example 5.1.

First, D is a peanut-shaped domain, and the boundary ∂D be

$$\mathbf{z}(\vartheta) = R_0 (4 \cos^2 \vartheta + \sin^2 \vartheta)^{\frac{1}{2}} (\cos \vartheta, \sin \vartheta)$$

with $R_0 = 0.5$. We fix the frequency by $\omega = 5$, $\mathbf{y}_0 = (4, -9)$. The parameterized surface impedance χ is given by

$$\chi(\vartheta) = \sin^4 \vartheta, \vartheta \in [\pi, 2\pi].$$

Table 1: The iterative steps and the regularization parameter.

Noise level	Iterative steps	Regularization parameter
0%	127	1.2019e-13
1%	128	9.7500e-02
5%	147	2.5117e-00

Second, D is a starfish-shaped domain, and the boundary ∂D be

$$\mathbf{z}(\vartheta) = (1 + 0.2 \cos 5\vartheta) (\cos \vartheta, \sin \vartheta).$$

We fix the frequency by $\omega = 3$, $\mathbf{y}_0 = (4, 9)$. The parameterized surface impedance χ is given by a constant function

$$\chi(\vartheta) = 1, \vartheta \in [\pi, 2\pi].$$

Table 2: The iterative steps and the regularization parameter.

Noise level	Iterative steps	Regularization parameter
0%	88	8.2341e-13
1%	98	2.5200e-02
5%	76	0.3063e-00

Figures 2 and 3 show the numerical reconstructions of the missing boundary and the impedance function with different noise levels $\delta \in \{0\%, 1\%, 5\%\}$ for the first and second case. We can see that the impedance function χ is sensitive depending on the noise level either for a function or for a constant function. The numerical reconstructions of the missing boundary are satisfactory. From table 1 and 2, we can also see that the number of the iterative steps using the noise data are not much more than using the exact data.

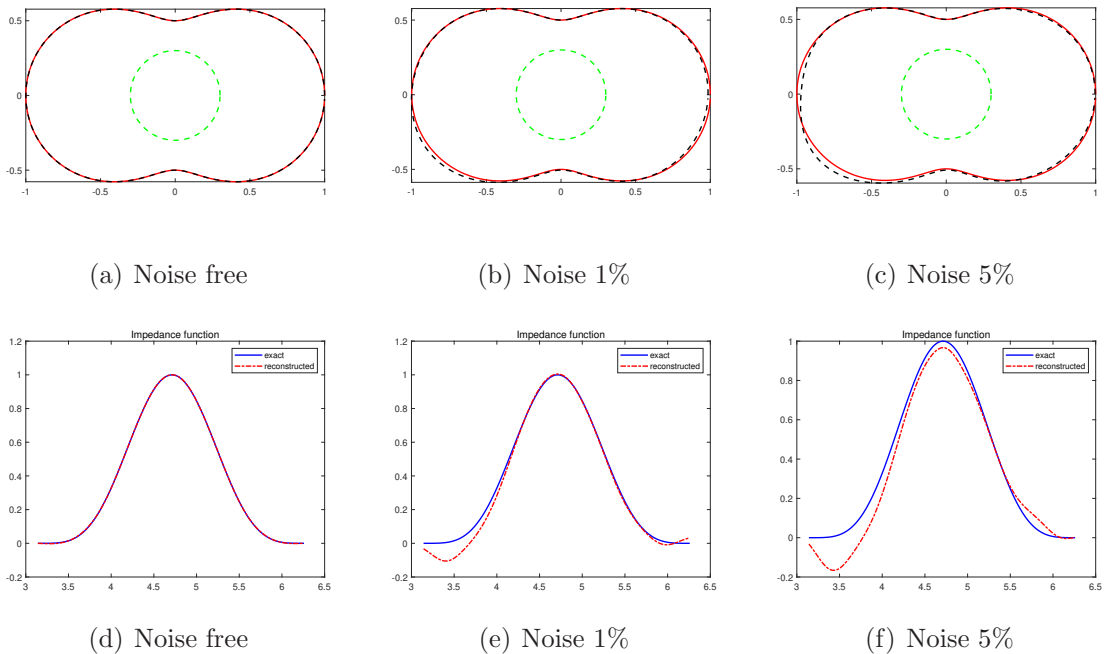


Figure 2: The numerical reconstructions of the shape and the impedance function χ with different noise levels $\delta \in \{0\%, 1\%, 5\%\}$ for peanut-shaped domain in Example 5.2.

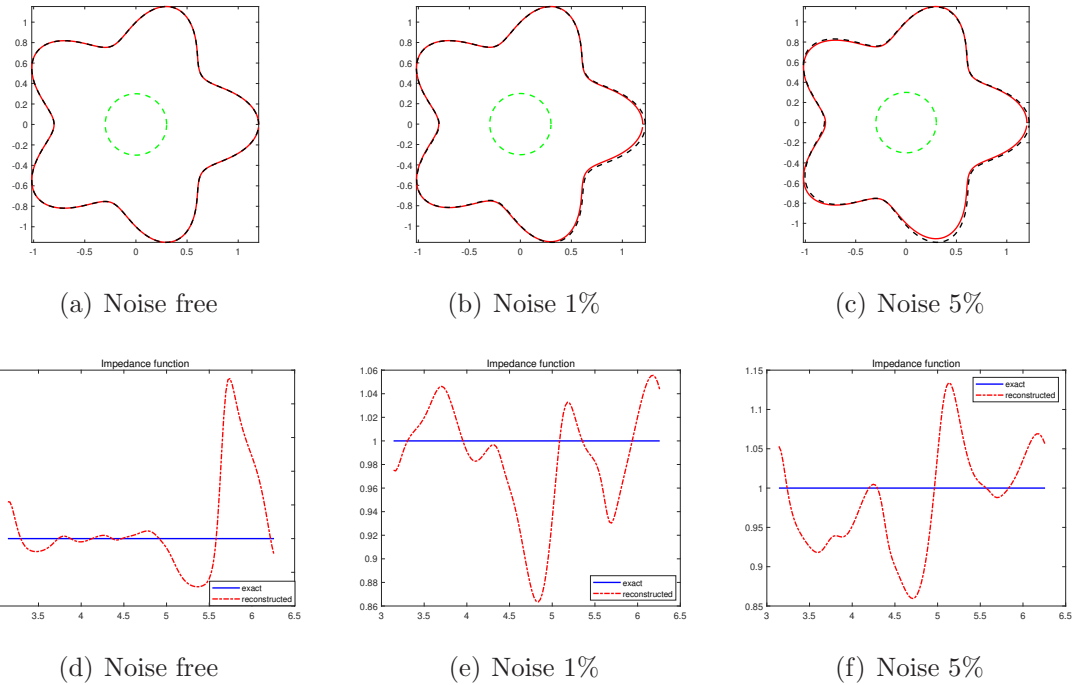


Figure 3: The numerical reconstructions of the shape and the impedance function χ with different noise levels $\delta \in \{0\%, 1\%, 5\%\}$ for the starfish-shaped domain in Example 5.2.

Example 5.3. In this example, we consider D be a circle, and its radius is 1.2. Consider the following boundary value problem

$$\begin{cases} \Delta u_p + \kappa_p^2 u_p = 0, & \text{in } D, \\ \Delta u_s + \kappa_s^2 u_s = 0, & \text{in } D, \\ T_n \mathbf{u} + i\omega \chi \mathbf{u} = \mathbf{g}, & \text{on } \partial D. \end{cases} \quad (5.1)$$

The impedance function χ is given by

$$\chi(\vartheta) = \sin^2 \vartheta, \quad \vartheta \in [0, 2\pi), \quad (5.2)$$

and the input boundary function $\mathbf{g}(\mathbf{x}) = (g_1, g_2)^\top$ is

$$g_1(\mathbf{x}(\vartheta)) = g_2(\mathbf{x}(\vartheta)) = \sin^2 \vartheta, \quad \vartheta \in [0, 2\pi). \quad (5.3)$$

In order to solve the inverse problem, we first get the Cauchy data $\mathbf{f} = \mathbf{u}|_{\Gamma_0}$ and $\mathbf{t} = T_n \mathbf{u}|_{\Gamma_0}$ by solving the direct problem (5.1). In this step, we use $\partial B = \{\mathbf{x} : |\mathbf{x}| = 3\}$. After this we use $\partial B = \{\mathbf{x} : |\mathbf{x}| = 7\}$ for solving the inverse problem. The initial guess of the boundary is a circle, and its radius is 0.6. The initial guess of the impedance function is a constant function $\chi_0 = 0.5$.

We fix the frequency by $\omega = 2$. The iterative steps and the regularization parameter chosen by Morozov discrepancy principle are given in Table 3. Figure 4 shows the numerical reconstructions of the missing boundary and the impedance function with different noise levels $\delta \in \{0\%, 1\%, 5\%\}$ for Example 5.3. We can see that the numerical reconstructions are satisfactory. From Table 3, we can also see that the number of the iterative steps using the noise data are not much more than using the exact data.

Table 3: The iterative steps and the regularization parameter.

Noise level	Iterative steps	Regularization parameter
0%	44	9.8186e-17
1%	47	1.0717e-05
5%	50	8.4172e-05

Example 5.4. As in example 5.3, we consider the same impedance boundary value problem. Different from the example 5.3, D is a peanut-shaped domain, and the boundary ∂D be

$$\mathbf{z}(\vartheta) = 0.5 (4 \cos^2 \vartheta + \sin^2 \vartheta)^{\frac{1}{2}} (\cos \vartheta, \sin \vartheta).$$

The initial guess of the boundary is a circle, and its radius is 0.3. The initial guess of the impedance function is a constant function $\chi_0 = 1$. We fix the frequency

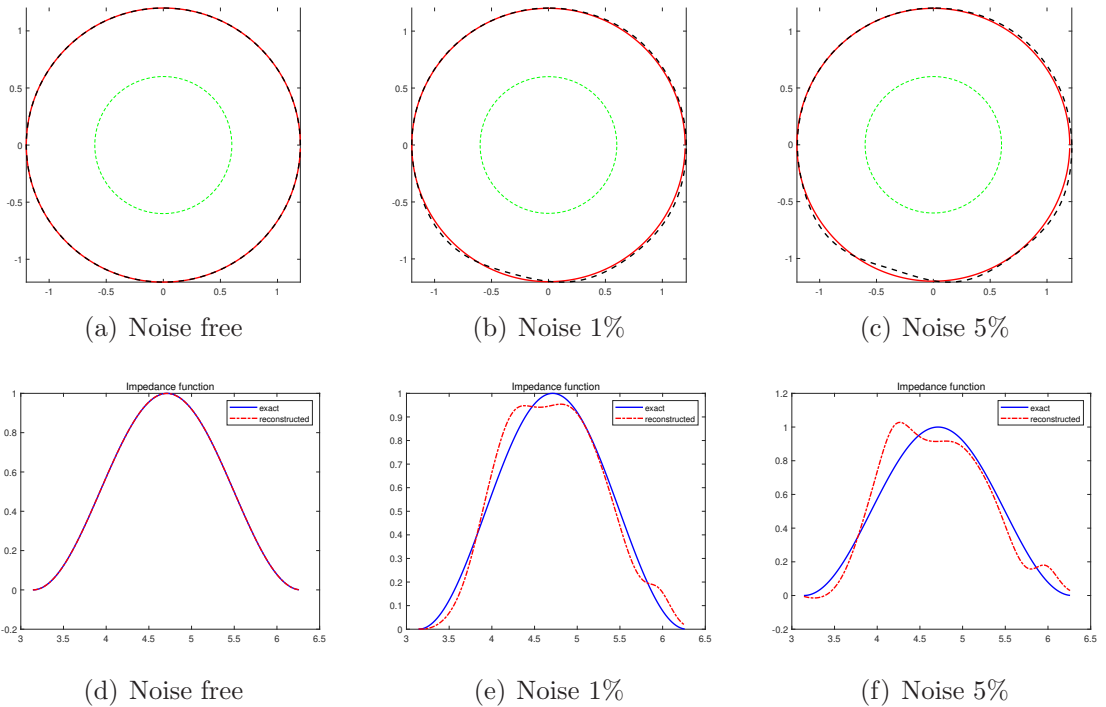


Figure 4: The numerical reconstructions of ∂D and the impedance function χ with different noise levels $\delta \in \{0\%, 1\%, 5\%\}$ in Example 5.3.

by $\omega = 1$. The iterative steps and the regularization parameter chosen by Morozov discrepancy principle are given in Table 4. Figure 5 shows the numerical reconstructions of the missing boundary and the impendence function with different noise levels $\delta \in \{0\%, 1\%, 5\%\}$ for Example 5.4. We can see that the numerical reconstructions are satisfactory. From Table 4, we can also see that the number of the iterative steps using the noise data are not much more than using the exact data.

Table 4: The iterative steps and the regularization parameter.

Noise level	Iterative steps	Regularization parameter
0%	11	1.5751e-15
1%	12	1.1075e-11
5%	13	2.2101e-10

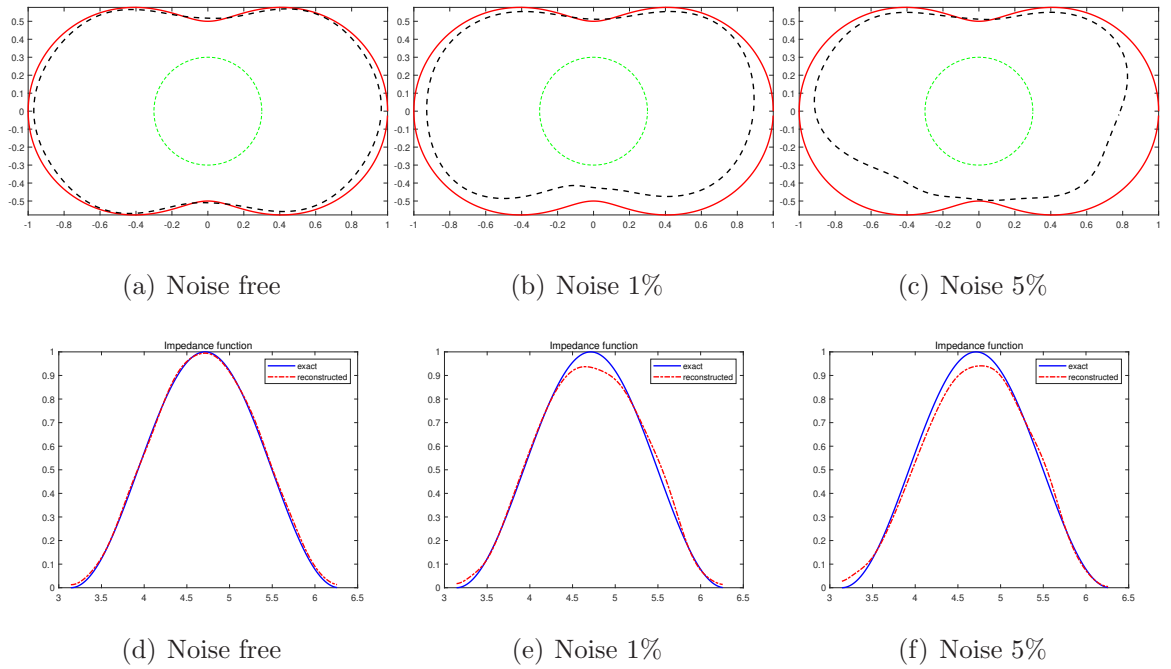


Figure 5: The numerical reconstructions of ∂D and the impendence function χ with different noise levels $\delta \in \{0\%, 1\%, 5\%\}$ in Example 5.4.

6 Concluding remarks

In this paper, we have studied the **inverse elastic problem** by a Newton-type iterative algorithm. This present problem is divided into two parts. The first part is to solve a Cauchy problem through using a integral equation method combining a regularization technique. The second part is simultaneously to recover the elastic impedance and the shape by a Newton-type iterative method. The effectiveness of the method has been shown by solving some examples. In the numerical examples, we construct the exact solution of the scattered field of the displacement to check the feasibility and accuracy of the presented method.

Acknowledgements

The research was supported by the Natural Science Foundation of China (No: 11501566) and Tianjin Education Commission Research Project (No: 2022KJ072).

ORCID iD

Yao Sun: <https://orcid.org/0000-0002-9165-1735>

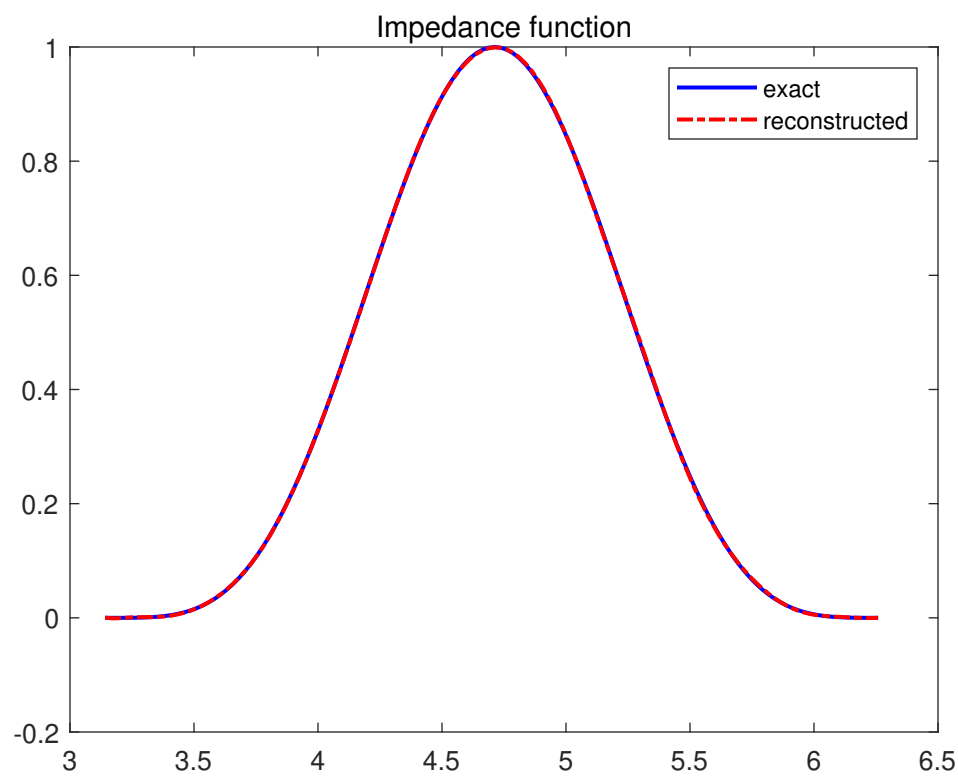
References

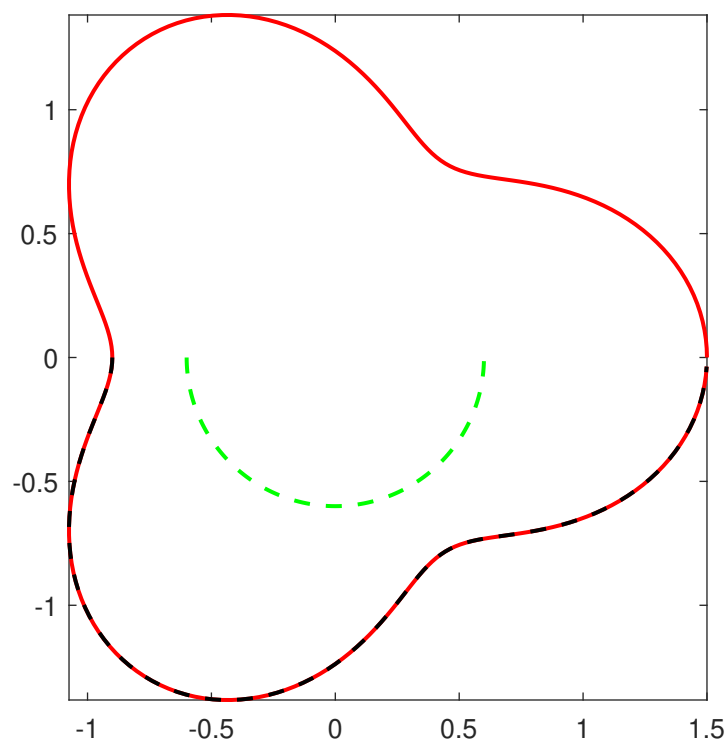
- [1] G. Alessandrini, A. Morassi and E. Rosset, Detecting cavities by electrostatic boundary measurements. *Inverse Problems*, 18(5):1333, 2002.
- [2] C. Alves and R. Kress, On the far-field operator in elastic obstacle scattering. *IMA Journal of Applied Mathematics*, 67:1–21, 2002.
- [3] H. Ammari, E. Bretin, J. Garnier, H. Kang, H. Lee and A. Wahab, In *Mathematical Methods in Elasticity Imaging*. Princeton University Press, 04 2015.
- [4] H. Ammari, E. Bretin, J. Garnier, H. Kang, H. Lee and A. Wahab, In *Theory of Elasticity*. 1986.
- [5] S. Andrieux, T. N. Baranger and A. B. Abda, Solving cauchy problems by minimizing an energy-like functional. *Inverse Problems*, 22:115 – 133, 2006.
- [6] D. Colton and R. Kress, *Inverse Acoustic and Electromagnetic Scattering Theory*, 4th edn (New York: Springer), 2019.
- [7] F. Cakoni and R. Kress, Integral equations for inverse problems in corrosion detection from partial cauchy data. *Inverse Problems and Imaging*, 1:229–245, 2007.

- [8] F. Cakoni, R. Kress and C. Schuft, Simultaneous reconstruction of shape and impedance in corrosion detection. *Methods and Applications of Analysis*, 17, 2010.
- [9] P. Deuflhard, H. W. Engl and O. Scherzer, A convergence analysis of iterative methods for the solution of nonlinear ill-posed problems under affinely invariant conditions. *Inverse Problems*, 14(5):1081, 1998.
- [10] H. Dong, J. Lai and P. Li, An inverse acoustic-elastic interaction problem with phased or phaseless far-field data. *Inverse Problems*, 36(3):035014, 2020.
- [11] H. Dong, J. Lai and P. Li, Inverse obstacle scattering for elastic waves with phased or phaseless far-field data. *SIAM Journal on Imaging Sciences*, 12(2):809–838, 2019.
- [12] H. W. Engl, M. Hanke and A. Neubauer. Regularization of inverse problems. 1996.
- [13] J. Elschner and M. Yamamoto, Uniqueness in inverse elastic scattering with finitely many incident waves. *Inverse Problems*, 26(4):045005, 2010.
- [14] D. Fasino and G. Inglese, Discrete methods in the study of an inverse problem for Laplace’s equation. *IMA Journal of Numerical Analysis*, 19(1):105–118, 1999.
- [15] S.N. Fata, B.B. Guzina, A linear sampling method for near-field inverse problems in elastodynamics. *Inverse Problems*, 20:713–736, 2004.
- [16] S.N. Fata, B.B. Guzina, Elastic scatterer reconstruction via the adjoint sampling method. *SIAM J. Appl. Math.* 67(5):1330–1352, 2007.
- [17] T. Hohage, *Iterative Methods in Inverse Obstacle Scattering: Regularization Theory of Linear and Nonlinear Exponentially Ill-Posed Problems*. PhD thesis, 1999
- [18] G. Hu, A. Kirsch and M. Sini, Some inverse problems arising from elastic scattering by rigid obstacles. *Inverse Problems*, 29(1):015009, 2013.
- [19] G. Hu, A. Mantile, M. Sini and T. Yin, Direct and inverse time-harmonic elastic scattering from point-like and extended obstacles. *Inverse Problems and Imaging*, 14(6):1025–1056, 2020.
- [20] P. Jakubik and R. Potthast, Testing the integrity of some cavity –the cauchy problem and the range test. *Applied Numerical Mathematics*, 58(6):899–914, 2008.
- [21] R. Kress, *Linear Integral Equations*, Springer-Verlag, Berlin, 1989.

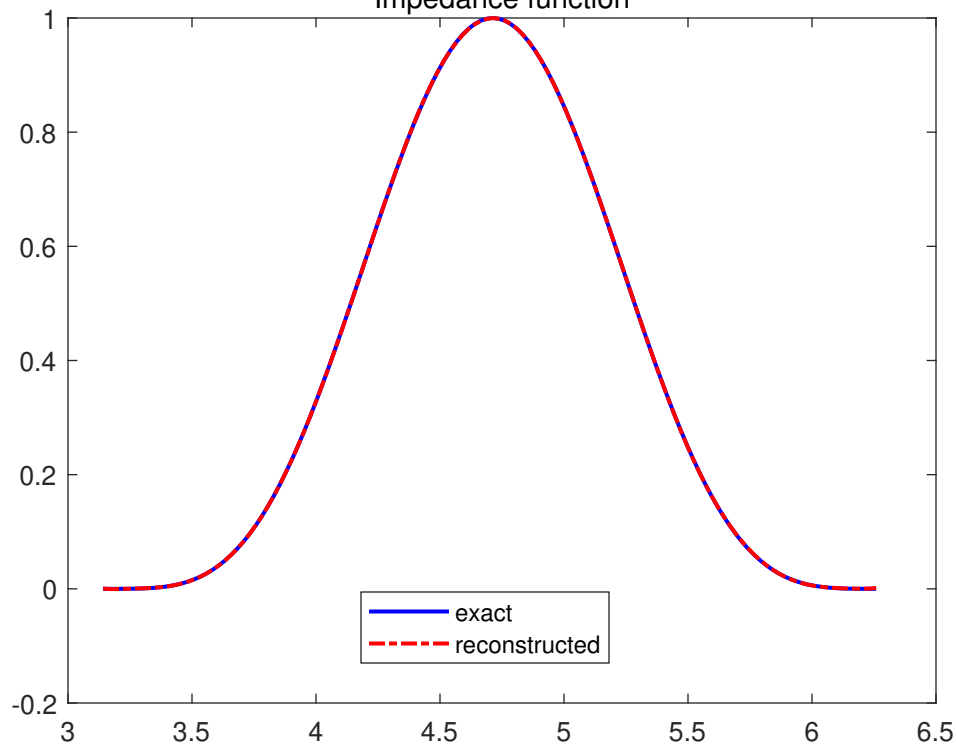
- [22] R. Kress, Uniqueness and numerical methods in inverse obstacle scattering. *Journal of Physics: Conference Series*, 73(1):012003, 2007.
- [23] V.D. Kupradze, *Three-dimensional problems of the mathematical theory of elasticity and thermoelasticity*. Amsterdam: North-Holland; 1979.
- [24] R. Kress, W. Rundell, Inverse scattering for shape and impedance, *Inverse Problems*, 17(4): 1075–1085, 2001.
- [25] R. Kress, W. Rundell, Inverse scattering for shape and impedance revisited, *Journal of Integral Equations and Applications*, 30(2):293–311, 2018.
- [26] Y. Liu, W. Jiang J. Yang, G. Li, The application of elastic impedance inversion in reservoir prediction at the jinan area of tarim oilfield. *Applied Geophysics*, pages 201–206, 2007.
- [27] J. Liu, X. Liu, J. Sun, Extended sampling method for inverse elastic scattering problems using one incident wave, *SIAM Journal on Imaging Sciences*, 12(2):874–892, 2019.
- [28] F.L. Louër, On the fréchet derivative in elastic obstacle scattering. *SIAM Journal on Applied Mathematics*, 72(5):1493–1507, 2012.
- [29] F. L. Louër, A domain derivative-based method for solving elastodynamic inverse obstacle scattering problems. *Inverse Problems*, 31(11):115006, 2015.
- [30] W. McLean, *Strongly Elliptic Systems and Boundary Integral Equations*, Cambridge: Cambridge University Press, 2000.
- [31] A. Morassi and E. Rosset, Stable determination of cavities in elastic bodies. *Inverse Problems*, 20(2):453, 2004.
- [32] Y. Sun, F. Ma, D. Zhang, An integral equations method combined minimum norm solution for 3D elastostatics Cauchy problem. *Comput. Methods Appl. Mech. Engrg.* 271, 231-252, 2014.
- [33] Y. Sun, F. Ma, X. Zhou, An Invariant Method of Fundamental Solutions for the Cauchy Problem in Two-Dimensional Isotropic Linear Elasticity. *J. Sci. Comput.*, 64, 197-215, 2015.
- [34] Y. Sun, L. Marin, An invariant method of fundamental solutions for two-dimensional isotropic linear elasticity. *Int. J. Solids Struct.* 117, 191-207, 2017.
- [35] Y. Sun, L. He, B. Chen, Application of neural networks to inverse elastic scattering problems with near-field measurements, *Electron. Res. Arch.*, 31(11), 7000-7020, 2023.

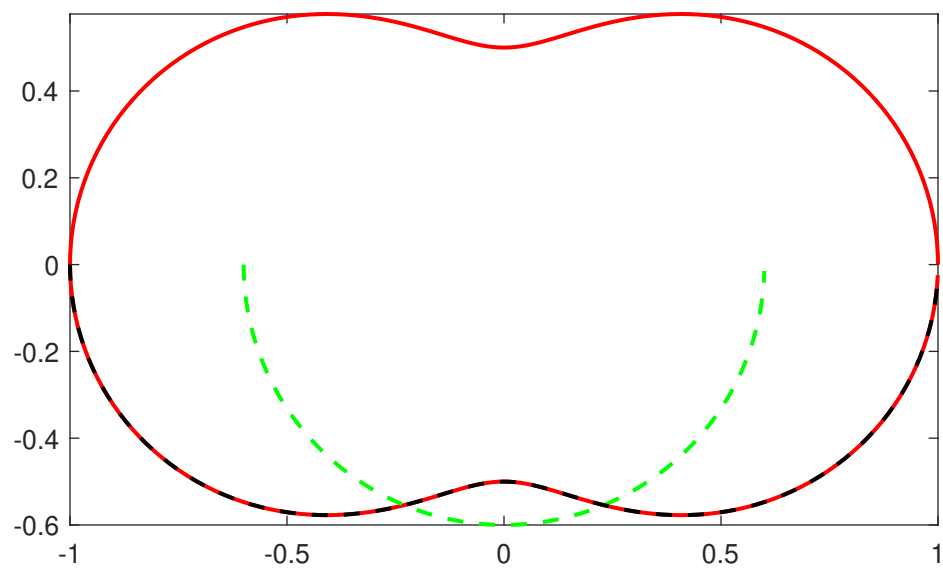
- [36] Y. Sun, P. Wang, X. Lu, B. Chen, A boundary integral equation method for the fluid-solid interaction problem, *Commun. Anal. Mech.*, 15(4): 716-742, 2023.
- [37] Y. Sun, X. Lu, B. Chen, The method of fundamental solutions for the high frequency acoustic-elastic problem and its relationship to a pure acoustic problem, *Eng. Anal. Bound. Elem.* 156(11), 299-310, 2023.
- [38] J. Zhang, Y. Wang, B. Xu, Q. Zhen and Y. Wu, Elastic impedance inversion based on improved particle swarm optimization. *Journal of Physics: Conference Series*, 1069(1):012042, 2018.

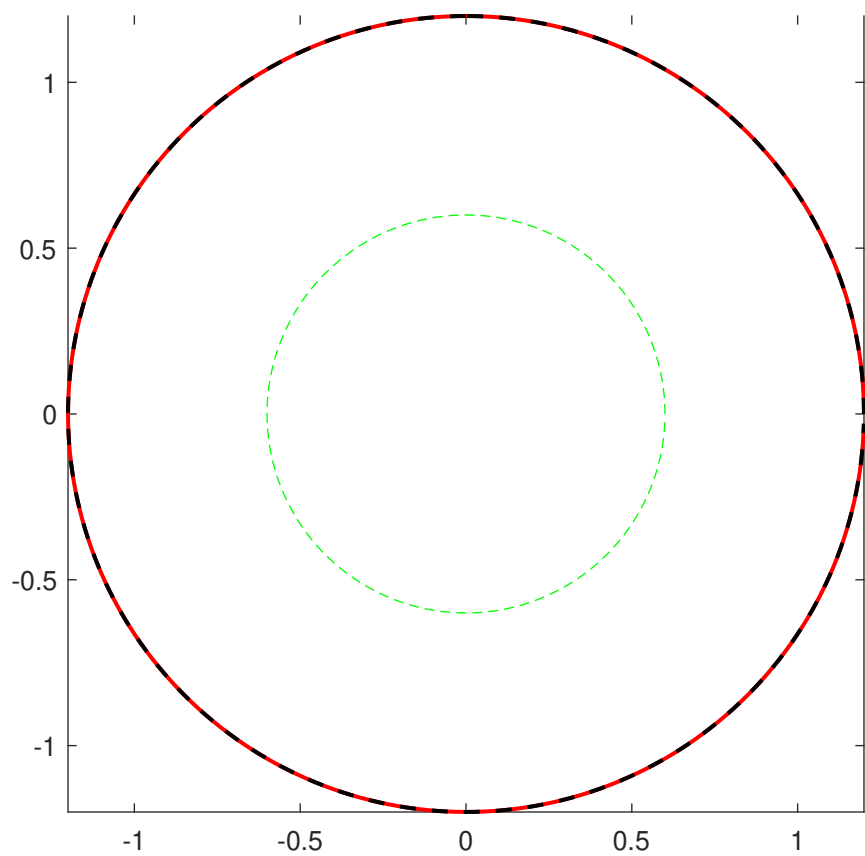


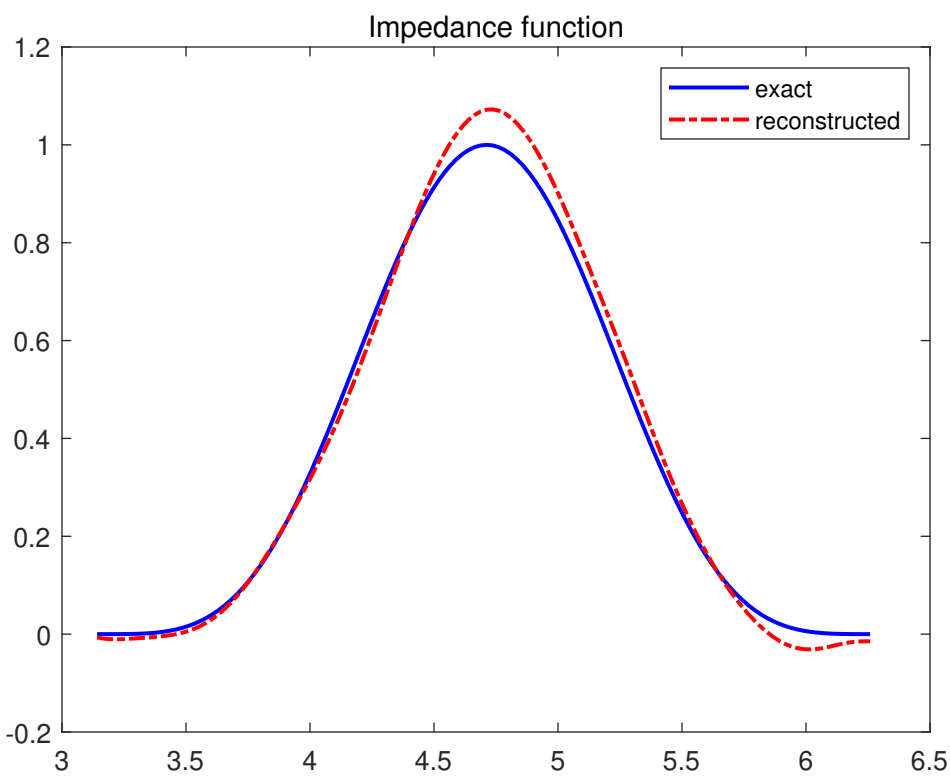


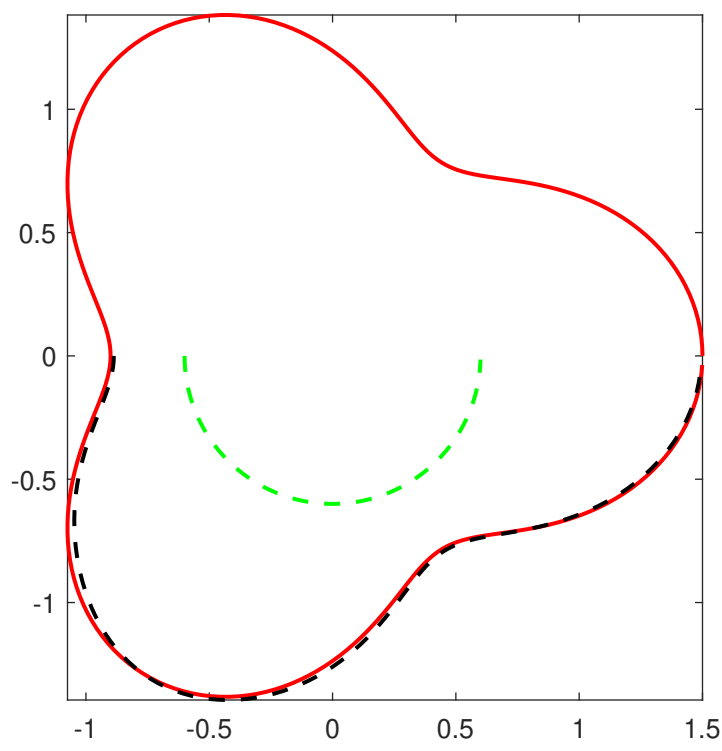
Impedance function

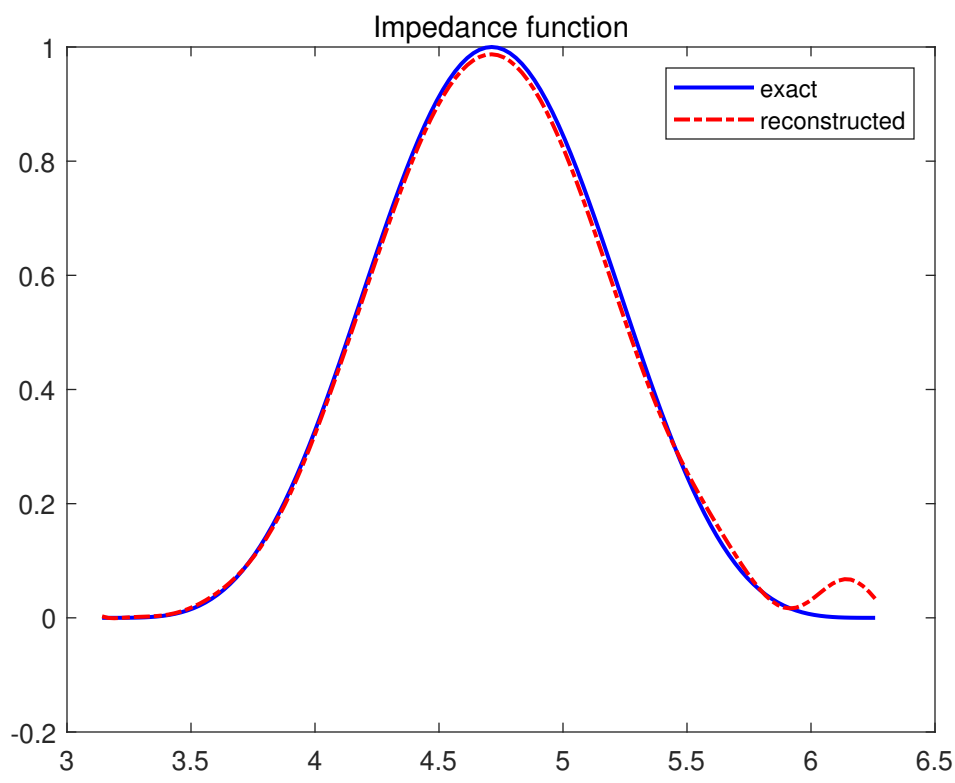


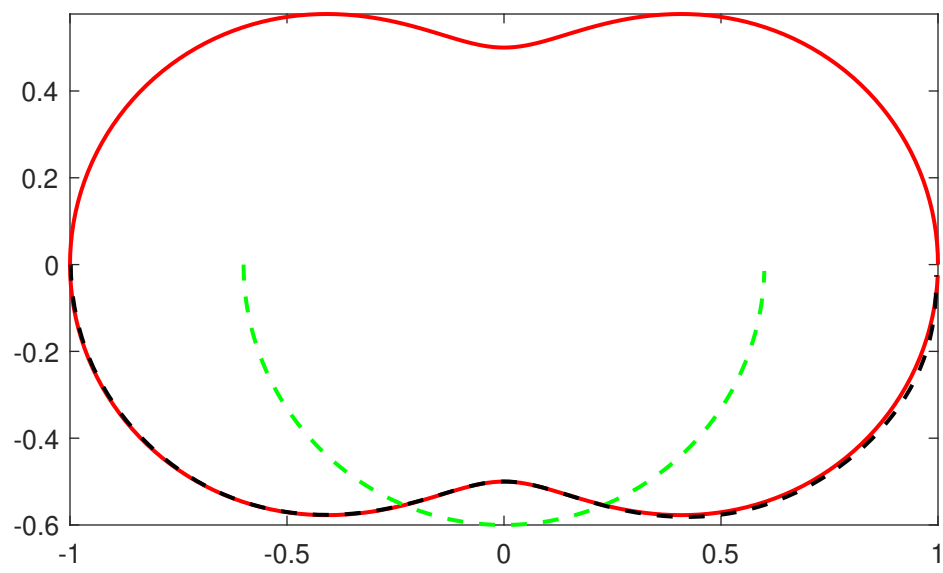


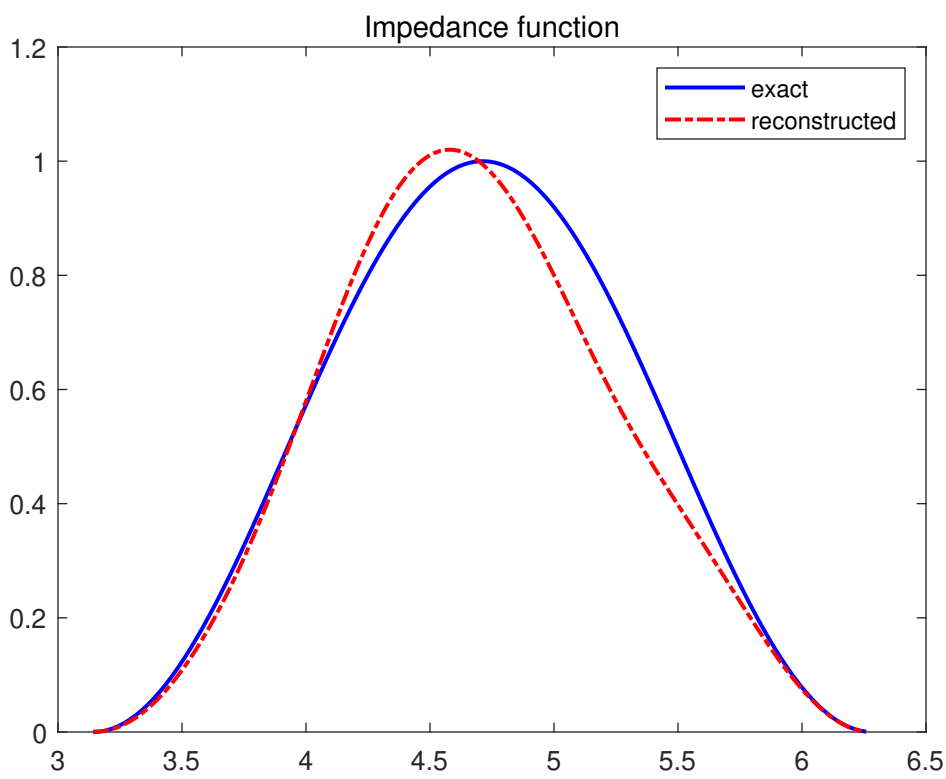


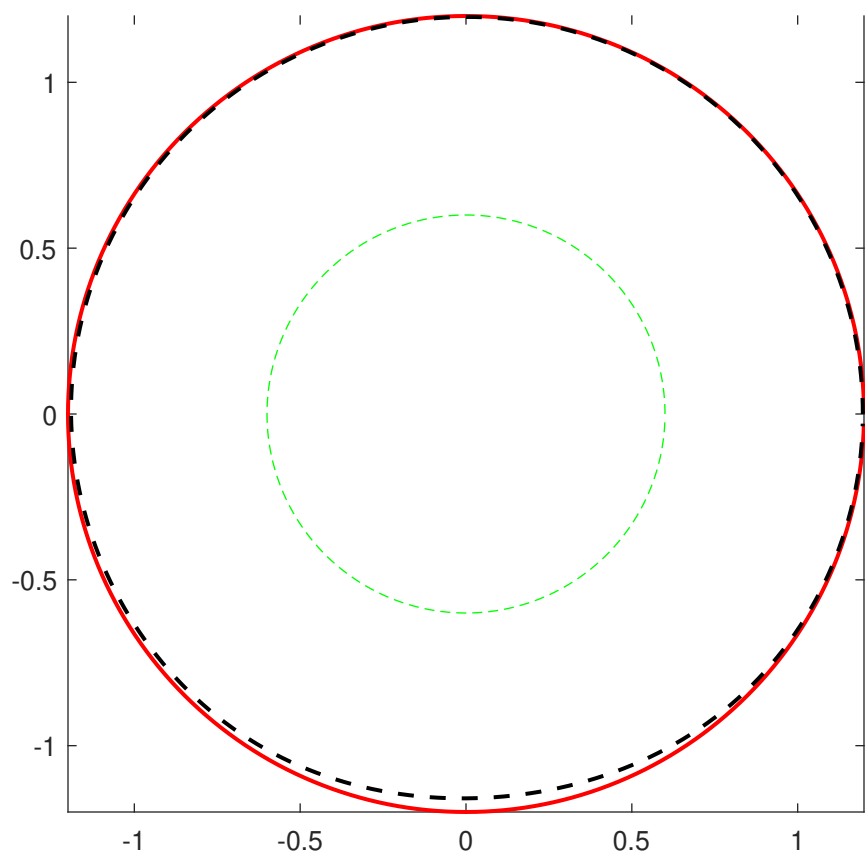


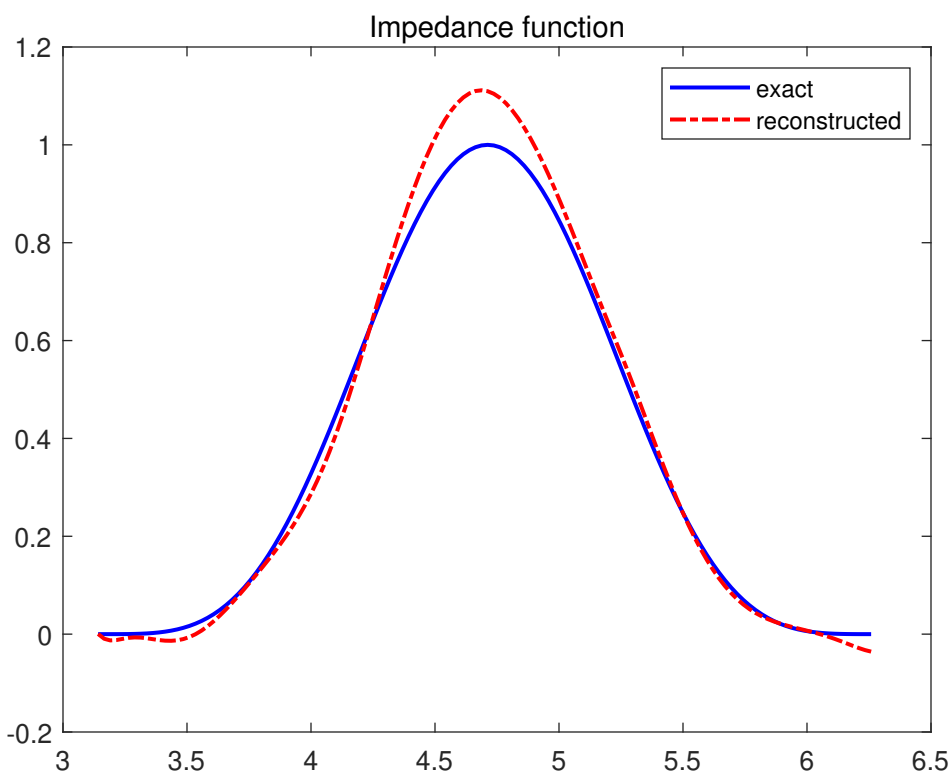


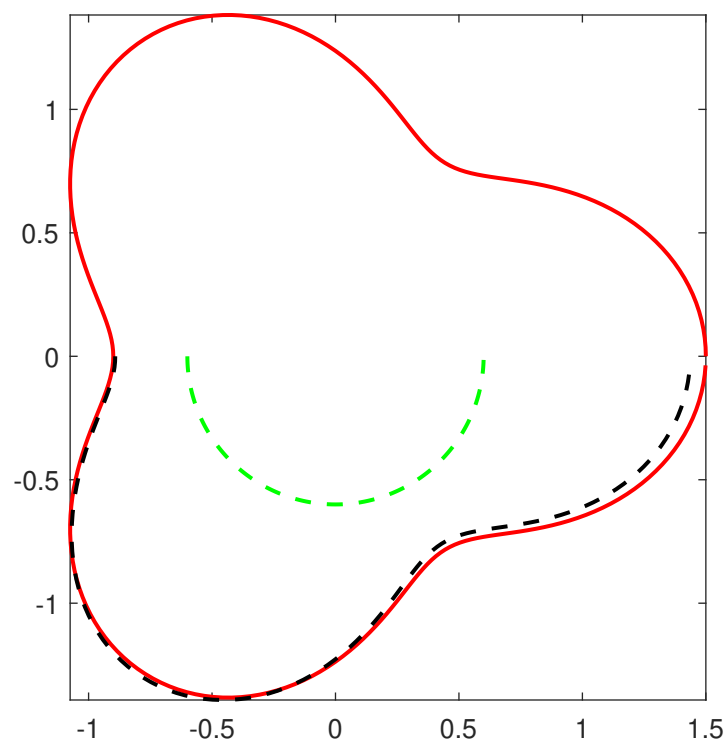


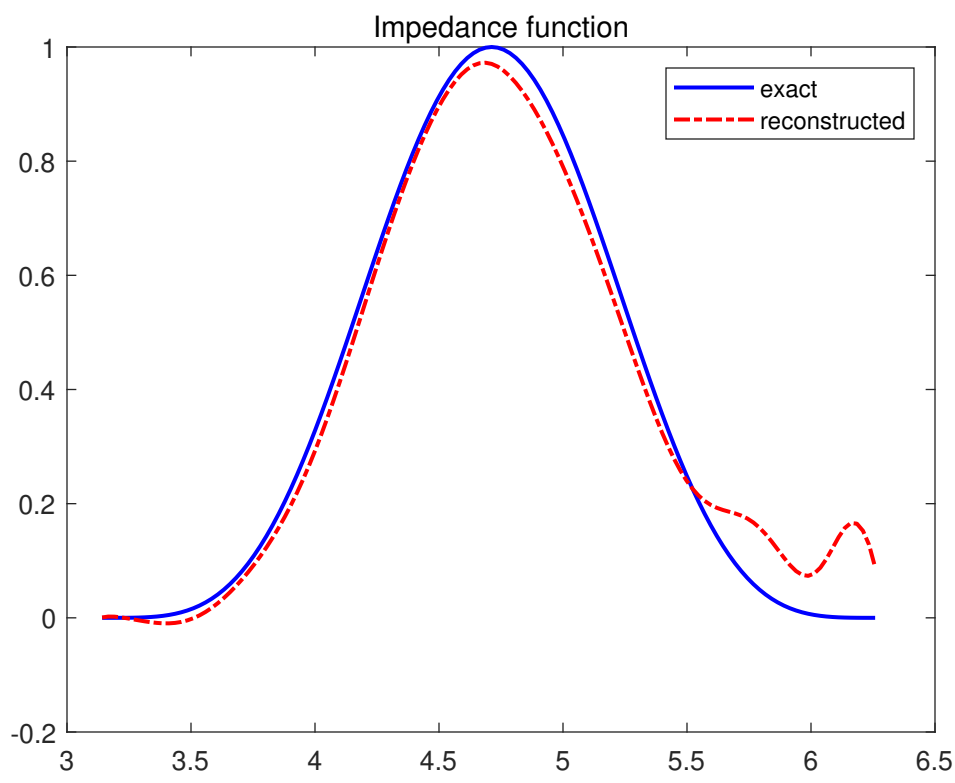


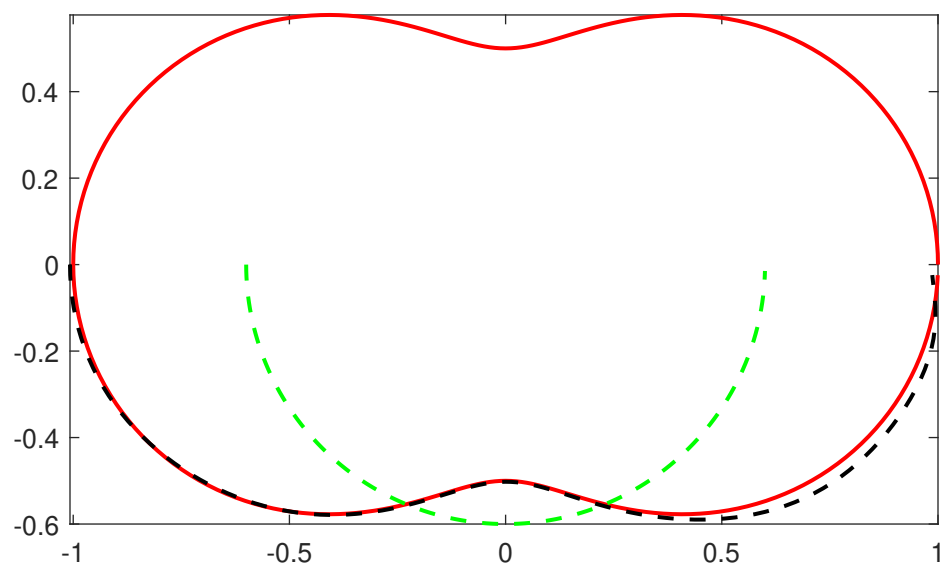


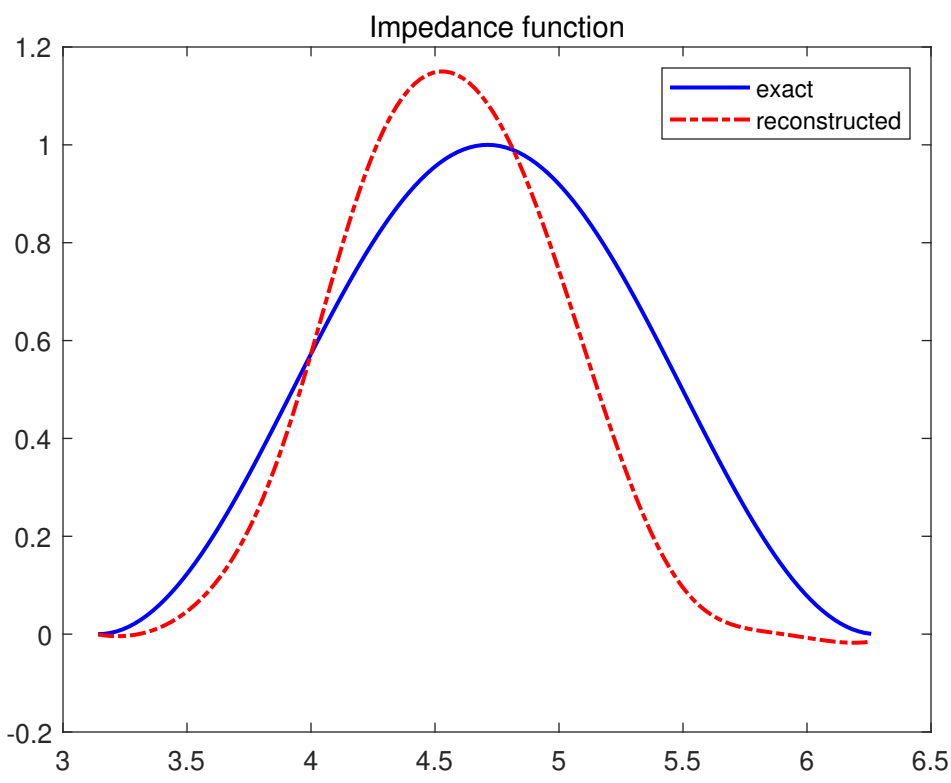


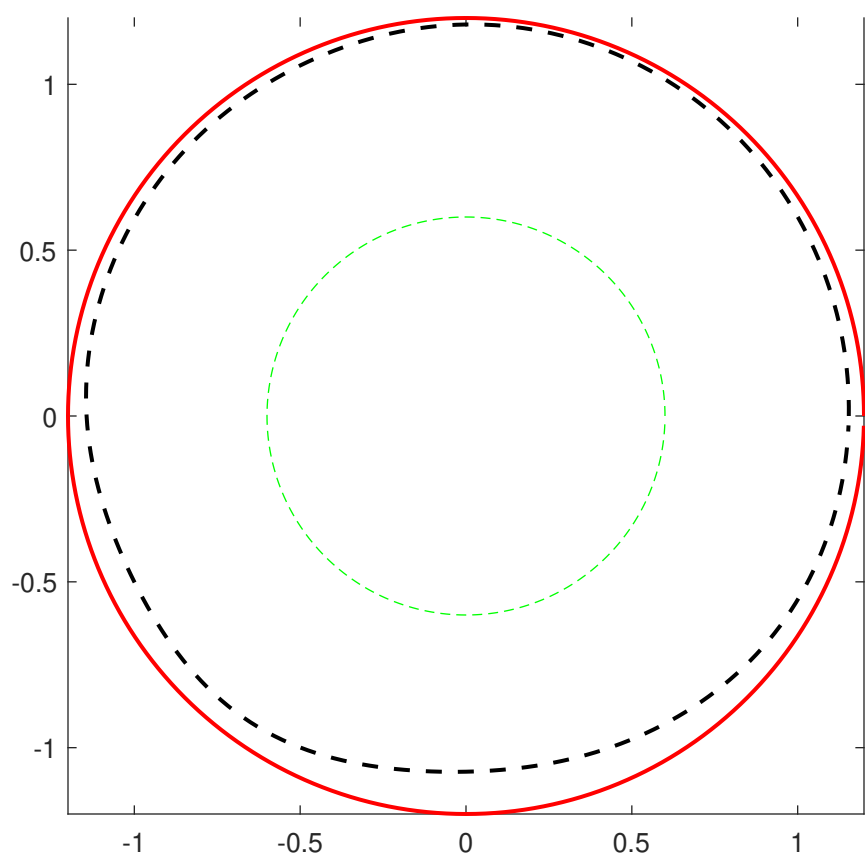


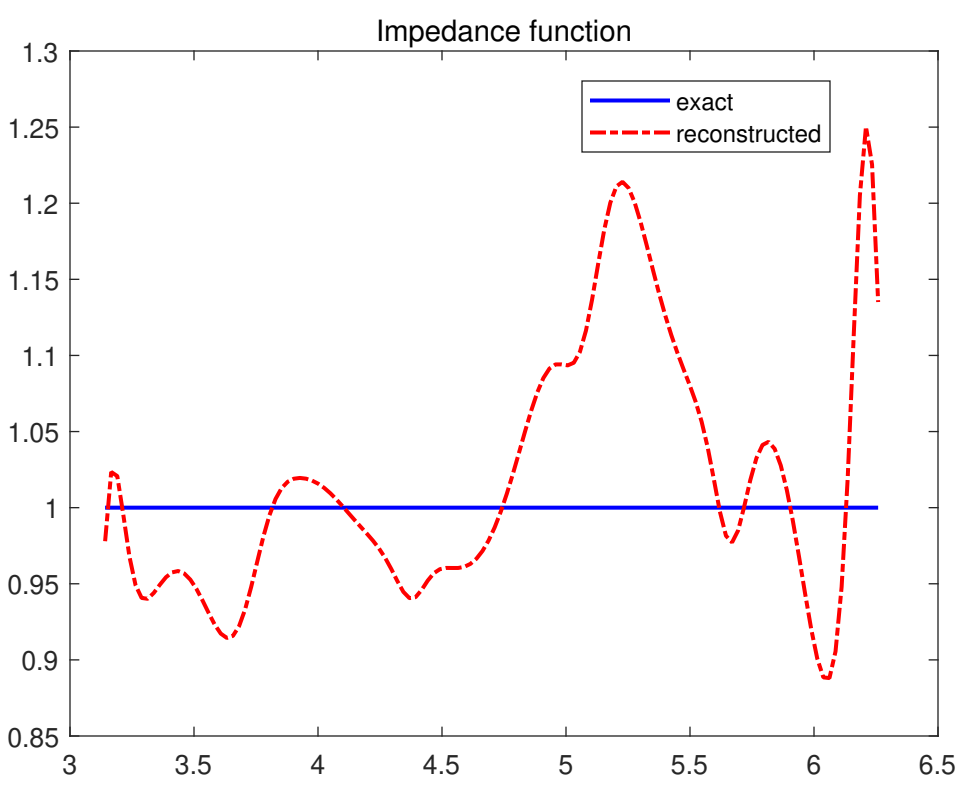


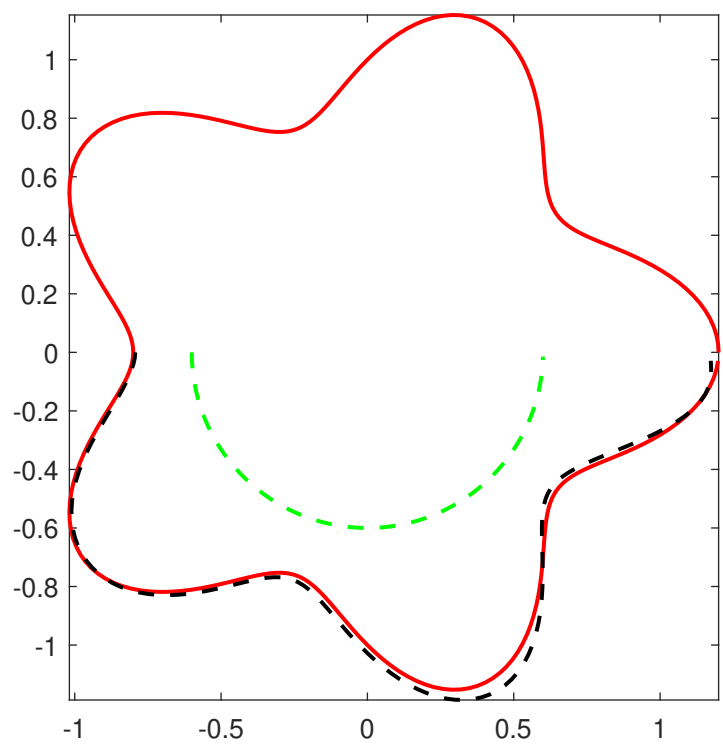












Impedance function

